RSC Advances

PAPER

View Article Online
View Journal | View Issue

Open Access Article. Published on 22 August 2025. Downloaded on 11/16/2025 4:40:19 AM.
This article is licensed under a Creative Commons Attribution-NonCommercial 3.0 Unported Licence.

Check for updates

Cite this: *RSC Adv.*, 2025, **15**, 30026

Hydroxyapatite-reinforced pectin hydrogel films PEC/PVA/APTES/HAp: doxycycline loading for sustained drug release and wound healing applications

Hirra Manzoor,[a] Nasima Arshad, *[a] Muhammad Anees Ur Rehman Qureshi[a] and Aneela Javed[b]

Doxycycline (DOXY)-loaded hydroxyapatite (HAp) pectin hydrogel films were prepared for sustained drug release and wound healing application. A series of pectin-based, DOXY-loaded hydrogels were synthesized *via* a solution casting method. HAp at varying amounts was used as a filler to synthesize PEC/PVA/APTES/HAp (PPC-5, -10, -15, -20) hydrogels. SEM, FTIR, TGA, and XRD analyses verified the porous morphology, structural integrity, thermal stability and amorphous nature of the hydrogels, respectively. A biodegradation study of the hydrogel was conducted using phosphate buffer saline (PBS) and proteinase-K enzymatic solutions. Cell viability was evaluated using the MTT assay with HEK293 cells. Moreover, drug-loaded hydrogel dressings were developed and subjected to *in vivo* wound healing studies on albino mice. Excision wound infliction was created to produce a 5–6 mm wide and 2–3 mm deep cutaneous wound. Swelling of the hydrogel films was found to be inversely related to the concentrations of HAp. The hydrogels exhibited significant swelling profiles in distilled water with a maximum swelling of 2519% in 140 min, while the highest swelling was observed at pH 6 in both buffer and non-buffer solutions. Antibacterial studies indicated bactericidal activity of hydrogels against both Gram-positive (*S. aureus*) and Gram-negative (*E. coli*) bacteria. *In vitro* release of DOXY from the hydrogel matrix (PPC-10) revealed 88.57% drug release in PBS solution within 3.5 h. Wound healing studies exhibited exceptional healing tendency, with complete excision wound healing achieved in 8 days. In conclusion, the remarkable biocompatible, biodegradable and nontoxic pectin-based hydrogel systems are suitable for drug delivery, tissue engineering, wound healing, and other medico-biological applications.

Received 21st March 2025
Accepted 4th August 2025

DOI: 10.1039/d5ra01989c

rsc.li/rsc-advances

1. Introduction

A significant challenge faced by the pharmaceutical sector in the 21st century is the growing demand for efficient, controlled, and targeted drug delivery systems that minimize side effects while enhancing bioavailability and therapeutic effectiveness.[1] The favorable properties of hydrogels have made them a viable material for numerous biomedical applications.[2] Hydrogels are 3D networks of natural or synthetic polymers that can absorb and retain a significant quantity of water without dissolving or losing structural integrity.[2,3] Their high porosity and water-attracting properties enable them to dramatically swell.[4] Hydrogels are widely recognized as an ideal choice for biomedical applications.[5] They are cost-effective and durable and possess tunable mechanical properties, allowing for adaptability in various applications. Additionally, their high swelling capacity and flexibility enhance their resemblance to living tissues.[3,6]

Hydrogels are classified based on their origin, structure, composition, crosslinking type, stimuli responsiveness, physical state, and electric charge, allowing for diverse applications in the biomedical and industrial fields.[4,7] Smart hydrogels respond to physical, chemical or biological stimuli by changing their physical state, swelling behavior or structure, thus triggering controllable responses such as drug release, shape change or mechanical adjustments.[8–10] Some common methods for hydrogel preparation are the solution casting method, physical cross-linking, free radical polymerization, chemical cross-linking, polyelectrolyte complexation and co-polymerization method.[10–12] The choice of synthesis technique has a prominent effect on the hydrogel's mechanical strength, biodegradability and swelling behavior. Certain properties, such as crosslinking density, polymer blend and processing

[a]Department of Chemistry, Allama Iqbal Open University, Islamabad, Pakistan. E-mail: nasimaa2006@yahoo.com; nasima.arshad@aiou.edu.pk

[b]Healthcare Biotechnology, Atta-ur-Rehman School of Applied Biosciences, National University of Sciences & Technology, Islamabad, Pakistan

© 2025 The Author(s). Published by the Royal Society of Chemistry

Open Access Article. Published on 22 August 2025. Downloaded on 11/16/2025 4:40:19 AM.
This article is licensed under a Creative Commons Attribution-NonCommercial 3.0 Unported Licence.

parameters, can be adjusted for various applications of hydrogels.[13]

Natural polymers, derived from bacteria (hyaluronic acid and dextran), plants (pectin, alginate, cellulose, and agarose) and animals (gelatin, collagen, and chitosan), are widely used for hydrogel preparation because of their promising properties, including their widespread availability, biocompatibility, low cost, biodegradability, bioavailability and eco-friendly nature.[14–16] Polysaccharides are a unique family of naturally occurring polymers that exhibit a wide diversity of structural characteristics. They consist of repetitive monomeric units linked together by glycosidic linkages to form long-chain carbohydrates.[17,18] Pectin is the most abundant and multifunctional cell wall component of all land plant peels.[19] It is a heterogenous polysaccharide that is a widely used functional food additive, as well as gelling agent.[20–22] Over the last few decades, pectin has been widely studied and used for drug delivery and other biomedical applications due to its favorable properties and behaviors, including gelation, reactivity, thickening, bioactivity and emulsifying properties.[23–25] The structure and chemical composition of pectin, which affects its properties and performances, changes with various parameters like the plant species, texture, extraction methods and storage conditions.[26–28] However, due to its multiple functional groups, pectin stands out as an excellent candidate for modifications.[29,30]

Despite the advantages, hydrogels based on natural polymers exhibit low mechanical strength, while synthetic polymers offer tailored properties and cost-effectiveness, but lack ecological benefits due to their non-biodegradability.[19,31] These issues can be resolved by mixing natural and synthetic polymers for hydrogel synthesis.[32,33] PVA is a white, odorless, water-soluble, flexible, granular, hydrophilic and biodegradable synthetic polymer with high mechanical strength that can be enhanced through cross-linking and good chemical resistance to solvents and oils. It is used as a stabilizer and thickener, as well as additive and coating adhesive.[33–35] Due to its chemical nature, unique combination of properties and simple production process, PVA is used in a variety of applications, ranging from simple consumer products to biomedical applications.[22,35]

Fillers are the materials that improve the thermal stability, strength and functional properties of the hydrogel, including its electrical and thermal conductivity, cytotoxicity, antibacterial activity and drug release.[36] The natural calcium phosphate mineral HAp ($Ca_5(PO_4)_3OH$) is commonly used as a filler in hydrogels due to its osteo-conductivity, bioactivity and biocompatibility. HAp is very similar to the mineral component found in bone. It is utilized as an inert filler in hydrogels, which increases the surface area and promotes drug loading/release profiles, while simultaneously enhancing the mechanical properties of the hydrogel. It also helps insoluble drugs dissolve more easily.[37] HAp improves the hydrogel's water retention and porosity, and also increases their mechanical properties, such as the compression resistance and stiffness.[38] A silane coupling agent, *e.g.*, APTES, is commonly used to functionalize surfaces with amine groups, enabling covalent bonding in hydrogel networks. APTES acts as a crosslinker, helping polymer matrices and inorganic substrates to generate stable siloxane (Si–O–Si) bonds. This improves the hydrogels' chemical stability, mechanical strength, and adhesion.[4]

DOXY (Fig. 1) is a broad-range antibiotic with only 50% bioavailability and belongs to the tetracycline class with broad-spectrum action against both Gram-positive and Gram-negative bacteria.[39] It has antioxidant, immunomodulatory, and anti-inflammatory qualities. It is used to treat cholera, malaria, STIs, traveler's diarrhea, intestinal, urinary, and respiratory tract infections, as well as chest and dental diseases. DOXY has also been studied as a treatment for certain cancers since some research indicates that it can prevent cell invasion and proliferation, trigger apoptosis, and stop the gap phase, which is when a malignant cell develops and gets ready to make DNA.[40] DOXY is mostly absorbed in the duodenum over the course of 2–3 h. According to reports, it has an 82–93% protein binding rate and a 0.7 L kg^{-1} volume of distribution. About 40–55.4% of a dose of DOXY is eliminated as the unaltered medication in the urine and feces.[41]

Structural and functional enhancements through cross-linkers and bioactive fillers have made multifunctional hydrogels promising candidates for various biomedical applications. This study focuses on designing pH-responsive, biodegradable and antibacterial pectin-based hydrogels with improved mechanical, swelling and therapeutic properties. In the present work, we have prepared a series of novel pectin-based HAp reinforced and APTES cross-linked PEC/PVA/APTES/HAp hydrogels by using the solution casting method. The hydrogels were characterized by FTIR, TGA, XRD, and SEM analyses, and further evaluated for cell viability, antibacterial activity, swelling behavior, and biodegradation studies. Furthermore, *in vitro* drug release and *in vivo* wound healing studies were done to evaluate their effectiveness for various biomedical applications. Despite extensive research on pectin-based hydrogels, the integration of APTES and HAp into a pectin-PVA matrix has not been explored yet in the literature, positioning this hydrogel as a novel and multifunctional platform for various biomedical applications. Pectin/PVA/APTES/HAp hydrogels are novel due to the unique combination of natural, synthetic and inorganic components, each contributing to enhanced the functionality. This unique formulation integrates the biocompatibility and gel-forming properties of pectin, the mechanical reinforcement of PVA, the functionalization capability of APTES and the osteoconductive nature of HAp, offering a multifunctional platform for drug delivery and wound healing applications. The synergistic interaction of these components enables enhanced structural stability, targeted bioactivity and controlled drug release, distinguishing it from previously reported pectin-based hydrogel systems. The literature review of similar studies on

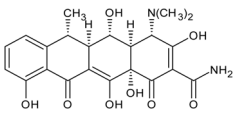

Fig. 1 The structural formula of DOXY.

Open Access Article. Published on 22 August 2025. Downloaded on 11/16/2025 4:40:19 AM.
This article is licensed under a Creative Commons Attribution-NonCommercial 3.0 Unported Licence.

pectin-based hydrogels for biomedical applications is provided in the SI (Table S1).

2. Experimental

2.1 Materials

Pectin (CAS No. 9000-69-5, MW: 60 000–130 000 g mol^{-1}, low methoxy content), APTES (CAS No. 919-30-2, M_w: 221.37 g mol^{-1}, 99%), PVA (CAS No. 9002-89-5, M_W: 146 000–186 000 g mol^{-1}), proteinase-K (CAS No. 39450-01-6, M_W: 28 930 g mol^{-1}), HAp (CAS No. 12167-74-7, Product No. 289396, M_W: 502.31 g mol^{-1}), potassium chloride (KCl, CAS No. 7447-40-7), calcium chloride ($CaCl_2$, anhydrous, CAS No. 10043-52-4), potassium dihydrogen phosphate (KH_2PO_4, 99%, CAS No. 9002-89-5) and sodium hydroxide (NaOH, CAS No. 1310-73-2) were purchased from Sigma-Aldrich, Germany. Hydrochloric acid (HCl, 37%, CAS No. 7647-01-0) and sodium chloride (NaCl, CAS No. 7647-14-5) were obtained from Merck, Germany. Methanol (CH_3OH, CAS No. 67-56-1, M_W: 32.04 g mol^{-1}) and ethanol (C_2H_5OH, CAS No. 64-17-5, M_W: 46.07 g mol^{-1}) were bought from BDH England. Disodium hydrogen phosphate ($Na_2HPO_4 \cdot 2H_2O$, CAS No. 7558-79-4) was bought from Scharlau, Spain. Sodium azide (NaN_3, M_W: 65.01 g mol^{-1}) and glycerin (CAS No. 56-81-5, MW: 92.09 g mol^{-1}) were obtained from Dabur, India Limited. HEK-293 cells were taken from the cell line bank of Atta ur Rehman School of Applied Biosciences (ASAB)l culture core. The model drug DOXY (MW: 444.4 g mol^{-1}) loaded on the hydrogels was purchased from a local company, Wilson's Pharmaceuticals Islamabad, Pakistan.

2.2 Synthesis of hydrogels

The solution casting method was employed to synthesize the PEC/PVA/APTES/HAp hydrogels.[42,43] PVA (0.5 g) and pectin (0.5 g) were individually dissolved in 40 mL and 50 mL of DW, respectively. The two polymer solutions were mixed and blended for two hours. In the next step, various concentrations of HAp clay were prepared by dissolving 5, 10, 15, and 20 mg, separately, in 10 mL of DW and sonicating for 30 min. It was then added to the mixture mentioned above and stirred for another hour. Additionally, 20 μL of APTES cross-linker was diluted using 10 mL methanol. The crosslinker solution was added dropwise to the original polymeric mixture. Finally, 20 μL of glycerin was added to avoid brittleness in hydrogels. This was followed by stirring for 1 h. Hydrogels were then obtained by pouring the solutions into Petri plates and permitting them to dry at room temperature. The dried hydrogels were designated as PPC (control), which is devoid of clay, and PPC-5, PPC-10, PPC-15, and PPC-20, which were each combined with 5, 10, 15, and 20 mg of HAp clay, respectively. Table 1 outlines the composition of the PEC/PVA/APTES/HAp hydrogels, detailing the specific proportions of each component used in their formulation.

2.3 Characterization of hydrogels

FTIR, TGA, XRD, and SEM were employed as material characterization techniques to analyze the synthesized hydrogels for their structure, stability, nature, and morphology. First, the anticipated characteristics of the hydrogel samples were examined using a FTIR spectrophotometer. The FTIR spectra of each hydrogel specimen was measured at a resolution of 2 cm^{-1} using triangular apodization. Hydrogel samples were vacuum-dried before going through the apparatus. Utilizing Thermo-Fisher Scientific's Nicolet iS10 spectrometer (Brookhaven, USA), the vacuum-dried hydrogels were scanned. The TGA model Q50 of Thermal Analysis (TA) Instrument (Newcastle, USA) was used to measure the thermal stability of the hydrogels. Five milligrams of hydrogel material were heated in an inert environment between 15 °C and 700 °C at a rate of 10 °C per minute in a platinum pan that was part of the apparatus. The study used an inert environment created by continuous nitrogen purging at a flow rate of 40 mL min^{-1}. The XRD instrument Xpert pro diffractometer, manufactured by PANalytical (Almelo, Netherlands), was used to investigate the nature of the synthesized hydrogels. The wavelength of the Cu Kα radiation employed in the aforementioned diffractometer was 1.544 Å. The 2θ operating range was 5°–80°, and the scan step size was 0.025°. The SEM analysis was performed on MIRA3 TESCAN (Brno, Czech Republic). The hydrogel specimen was attached to carbon conductive tape and coated with tungsten for 92 seconds at a rate of 0.8 nm s^{-1} using the Safematic CCU-010 sputter coater. The samples were then inspected at various magnifications.

Table 1 Compositions of the synthesized PEC/PVA/APTES/HAp hydrogel series

	Composition				
Hydrogels	Pectin (g)	PVA (g)	APTES (μL)	HAp (mg)	DOXY (mg)
PPC (control)	0.5	0.5	20	0	—
PPC-5	0.5	0.5	20	5	—
PPC-10	0.5	0.5	20	10	—
PPC-15	0.5	0.5	20	15	—
PPC-20	0.5	0.5	20	20	—
DPPC	0.5	0.5	20	10	50

2.4 *In vitro* biodegradation analysis

The hydrogel biodegradation rate was investigated using PBS and proteinase-K enzymatic solutions. The biodegradation percentage was computed using eqn (1).

$$\text{Biodegradation}(\%) = \frac{W_o - W_t}{W_o} \times 100 \quad (1)$$

W_o is the initial weight of the hydrogel specimen, and W_t is the weight of the sample taken out of PBS and proteinase-K solutions at pre-arranged intervals (after the surface water has been removed). Pre-weighed hydrogels were added to 25 mL of PBS. Samples were removed on the 1st, 3rd, 7th, 10th, 14th, and 21st days. Weight loss was calculated by subtracting the initial and final weights, with the process conducted at room temperature without stirring. On the other hand, 0.2 mg mL^{-1} proteinase-K was made in PBS, followed by the addition of

 © 2025 The Author(s). Published by the Royal Society of Chemistry

Open Access Article. Published on 22 August 2025. Downloaded on 11/16/2025 4:40:19 AM.
This article is licensed under a Creative Commons Attribution-NonCommercial 3.0 Unported Licence.

0.29 g $CaCl_2$. As a precaution to prevent the growth of microbes, 0.01% w/v NaN_3 was added. The enzymatic solution was then supplemented with a pre-weighed, precisely determined amount of hydrogel. After that, the samples were placed in an incubator set at 37 °C. The weight loss was calculated by comparing the weight of the dried and incubated gels on the first, third, and seventh days.

2.5 *In vitro* cell viability assay

The sterilization protocol was followed prior to this assay. The hydrogel samples were evaluated for cell viability using the MTT assay with HEK-293 cells. HEK-293 cells were grown in Dulbecco's Modified Eagle Medium (DMEM). A total of 1×10^4 cells were plated with 2 mg of hydrogel and incubated at 37 °C. The hydrogel-free cells served as a reference group. A Bio-Rad (Washington, DC, USA) absorbance microplate reader model PR4100 was used to measure absorbance after 48 h. Furthermore, by performing the cell line experiments in triplicate, the cell viability was computed using eqn (2).

$$\text{Cell viability}(\%) = \frac{\text{Sample absorbance}}{\text{Reference absorbance}} \times 100 \quad (2)$$

2.6 *In vitro* swelling analysis

Swelling experiments were performed to confirm the swelling characteristics of each hydrogel. 10 mg of dry hydrogel was submerged in DW, and the swelling hydrogel's weight was measured on a regular basis. The excess solvent in the beaker was wiped away using tissue paper before weighing the hydrogel. The ability of each hydrogel to swell was also evaluated in the same stream in buffer and non-buffer solutions at pH values of 2, 4, 6, 7, 8, and 10. Similarly, NaCl and $CaCl_2$ solutions of 0.2, 0.4, 0.6, 0.8, and 1 M were used to investigate the impact of the electrolyte type and concentration on the swelling of the generated hydrogels. The ability of each hydrogel to swell was ascertained using the following eqn (3).

$$\text{Swelling}(\%) = \frac{W_s - W_d}{W_d} \times 100 \quad (3)$$

where W_s and W_d stand for the swelling hydrogel and dried hydrogel, respectively. The diffusion mechanism of water or solvents entering and exiting the hydrogels may be explained using eqn (4).

$$F = kt^n \quad (4)$$

where "F" represents fractional swelling, "k" the swelling rate constant, "t" the swelling time, and "n" the swelling exponent. As water or a solvent enters a hydrogel framework, the various diffusion processes that take place are characterized by the values of "n."

2.7 *In vitro* antibacterial activity

The antibacterial activity was evaluated against *S. aureus* (Gram-positive) and *E. coli* (Gram-negative) stains using the disc diffusion technique. The tested bacteria were cultivated on sterilized Petri plates, and then inoculated with LB (1% NaCl, 1% trypton, and 0.5% yeast) at a pH of 7.4.60 μL of the generated bacterial culture was put on agar plates containing 1.5% agar and LB medium. An ethanol-clean glass spreader was utilized to uniformly distribute the spilled culture across the LB agar plates. Subsequently, hydrogel samples (5 mg) were added to the LB agar plates, which were then incubated with the bacterial lawn at 37 °C. After 24 h, the I_z values were measured using a zone reader scale with a minimum increment of 1 mm. The "0" reading on the zone reader was positioned at the center of the circle. The distance from the center to the edge of the circular area was referred to as the zone of inhibition, and was recorded in millimeters.

2.8 *In vitro* drug loading and release studies

In vitro drug release experiments were conducted under physiological conditions (pH 7.4 and 37 °C) in PBS solution. 1 M PBS solution (pH 7.4) was prepared by dissolving 8, 1.44, 0.24, and 0.2 grams each of NaCl, Na_2HPO_4, KH_2PO_4, and KCl in sterilized DW (autoclaved). Taking into account of the compromising results of swelling, biodegradation and cell viability analyses of the hydrogels, DOXY (100 mg) was loaded on the PPC-10 hydrogel. Pectin (0.5 g) and PVA (0.5 g) solutions were prepared in 50 and 40 mL of DW, respectively. After blending both solutions for two hours, HAp (10 mg) was added. To make the DOXY-loaded DPPC, 50 mg of DOXY was combined with 20 mL of DW and put into a PEC/PVA/HAp mixture before the addition of 20 μL of APTES cross-linker and 20 μL of glycerin. In PBS, the DOXY release pattern was estimated. After drying, the DOXY-loaded DPPC was added to 200 milliliters of PBS solution. A 5 mL solution was then taken every 10 min and exposed to the UV-visible spectrophotometer at a wavelength of 275 nm. As a reference, a recently made PBS solution was used. To calculate the released amount of DOXY, a calibration curve was employed. The following empirical models from eqn (5)–(7) were also used to study the drug release mechanism and kinetics:[43]

$$M_t = M_o + K_o t \text{ (Zero order model)} \quad (5)$$

$$\ln\frac{M_t}{M_o} = n\ln t + \ln k \text{ (Korsmeyer} - \text{Peppas model)} \quad (6)$$

$$\text{ft} = Q = K_H \times t^{1/2}\text{(Higuchi model)} \quad (7)$$

where M_t is the amount of drug released at time t, whereas M_o is the total amount of drug loaded. K_H, K, and K_o are the rate constants.

2.9 *In vivo* wound healing studies

2.9.1 Ethical approval. The guidelines set forth in European Community Council Directive 2010/63 were followed while handling each animal involved in the *in vivo* study. The experimental protocol (No. F.1-5/ERC/2024) was reviewed and approved by Institutional Ethics Committee for Animal Care and Experimentation (IECACE), NIH Islamabad, Pakistan. Each *in vivo* experiment was carried out according to the guidelines and internationally accepted norms.

Open Access Article. Published on 22 August 2025. Downloaded on 11/16/2025 4:40:19 AM.
This article is licensed under a Creative Commons Attribution-NonCommercial 3.0 Unported Licence.

2.9.2 Cutaneous wound animal model. For the wound healing analysis, 30 female albino mice, weighing between 18 and 25 grams, were purchased. The animals were housed at NIH, Islamabad, with a temperature of 25 ± 2 °C and a relative humidity of 45 ± 5 °C throughout the wound healing procedure. The animals were given unlimited access to food and water, and were given seven days to acclimate to their surroundings before the start of the experiment. Animals were randomly divided into three groups containing ten mice in each group. For each group, the age and weight were roughly the same.

Group A: Control group (only pyodine was applied daily on the wound).

Group B: PPC-10 group (blank PPC-10 hydrogel was applied on the wound).

Group C: DPPC group (DOXY-loaded DPPC hydrogel was applied on wound).

2.9.3 Excision wound infliction. Mice were anesthetized by intraperitoneal injection of xylazine (10 mg kg^{-1}) and ketamine hydrochloride (100 mg kg^{-1}). The animals were shaved dorsally using an electric clipper, and a circular stainless-steel stencil was used to mark the region of the wound with methylene blue. A medical blade, sharp scissors and toothed forceps were used to produce an excision wound that was 5–6 mm wide and 2–3 mm deep along the markings. Post-operative care was guaranteed, and all surgical procedures were done under sterile conditions. The animals received treatment once every day.

2.9.4 Wound assessment. Every day, measurements of the wound area in the excision model and digital photographs were taken. Transparent graph paper was used to measure the healed wound. The percentage of wound contraction was used to assess each group's wound healing activity. The following formula was used to determine the proportion of wound contraction, eqn (8):

$$\text{Wound contraction } (\%) = \frac{\text{Wound area on day0} - \text{Wound area on day } n}{\text{Wound area on day0}} \times 100 \quad (8)$$

where n represents the number of days, like the 2nd, 3rd, 4th, 6th, and 7th day. Three animals or more were employed for each measurement of the wounds' surface area. The acquired results were presented as the mean ± standard error of the mean.

2.10 Statistical analysis

Origin Pro (8.5.1), created by Origin Lab Corporation in the United States, was utilized to analyze the data statistically by one-way ANOVA. The evaluation of the swelling and kinetic parameters for drug release from hydrogels was also performed using linear fitting. Three independently conducted experiments provided the antibacterial and cytocompatibility data, which were presented as the mean ± SD.

3. Results and discussion

3.1 Scheme of synthesis

The anticipated scheme for the HAp-incorporated PEC/PVA/APTES/HAp hydrogel for *in vitro* drug delivery and *in vivo* wound healing applications is depicted in Fig. 2. The dotted and bold lines represent the physical and chemical interactions formed between the functional groups of the various components, highlighting the structural integration and bonding within the system. Pectin and PVA form the primary hydrogel network through hydrogen bonding, providing a flexible and biocompatible matrix. APTES acts as a silane coupling agent, introducing amine groups that facilitate covalent bonding with both the polymeric matrix and HAp particles, enhancing the network stability and crosslinking density. HAp is uniformly dispersed within the matrix, and interacts with both the functionalized polymers and loaded drug molecules *via* ionic and hydrogen bonding. Together, these interactions create a cohesive and multifunctional structure capable of sustained drug release, mechanical integrity and wound healing.

3.2 Characterization of hydrogels

3.2.1 FTIR analysis. The structural modifications and associations between the different components of the synthesized hydrogels were verified by FTIR analysis. The FTIR spectra of pure pectin, PVA, APTES and HAp are shown in Fig. 3(a). Pectin exhibited distinctive absorption peaks at 3280–3600 cm^{-1} and 1025 cm^{-1} for –OH stretching and bending vibrations, respectively. The polymer-linked C–H stretching and bending vibrations are responsible for the absorption peaks observed at 2920 cm^{-1} and 1490 cm^{-1}. In addition, the stretching peaks of C=O, COO^-, C–O–C and CH–OH in the aliphatic cyclic secondary alcohol were observed at 1740 cm^{-1}, 1634 cm^{-1}, 1072 cm^{-1} and 1139 cm^{-1}, respectively.[44] The –OH stretching band was shown by PVA in the 3200–3550 cm^{-1} range. Peaks at 2910 cm^{-1}, 1428 cm^{-1} and 1094 cm^{-1} are caused by C–H stretching, $-CH_2$ wagging and C–O stretching vibrations, respectively.[45] APTES peaks at 2973 cm^{-1} and 2883 cm^{-1} represent asymmetric and symmetric C–H stretching, respectively. The stretching vibrations for C–O, Si–O and C–N appeared at 1094 cm^{-1}, 1000–1100 cm^{-1}, and 1441 cm^{-1}, respectively. CH_2 bending or wagging modes appeared at 1389 cm^{-1}. The existence of amine, alkyl, ethoxy and silane functionalities in APTES is confirmed by these peaks.[46] In HAp FTIR, the phosphate (PO_4^{3-}) groups are represented by peaks at 1024 cm^{-1}, 960 and 872 cm^{-1}, corresponding to their symmetric stretching, asymmetric stretching and bending vibrations, respectively. The presence of carbonate ions is suggested by peaks around 1417 cm^{-1} and 1422 cm^{-1}.[47]

Fig. 3(b) shows the FTIR spectra of the PPC hydrogels, which show the fundamental peaks of pectin, PVA, APTES and HAp. The stretching peak seen in the 3100–3650 cm^{-1} area is attributed to the presence of –OH groups in PVA and pectin. The –OH group was involved in both intra- and inter-molecular hydrogen bonding inside the hydrogel matrix, as demonstrated by the peak broadening.[48] Furthermore, –OH bending vibrational peaks were also observed at 1329 cm^{-1}. The C–H stretching vibrations were represented by the band that appeared at 2940 cm^{-1}. The bands for C=O, C–O–C, COO^-, CH–OH in pectin appeared in the hydrogel at 1730 cm^{-1}, 1086 cm^{-1}, 1645 cm^{-1} and 1145 cm^{-1}, respectively. The characteristic

 © 2025 The Author(s). Published by the Royal Society of Chemistry

Open Access Article. Published on 22 August 2025. Downloaded on 11/16/2025 4:40:19 AM.
This article is licensed under a Creative Commons Attribution-NonCommercial 3.0 Unported Licence.

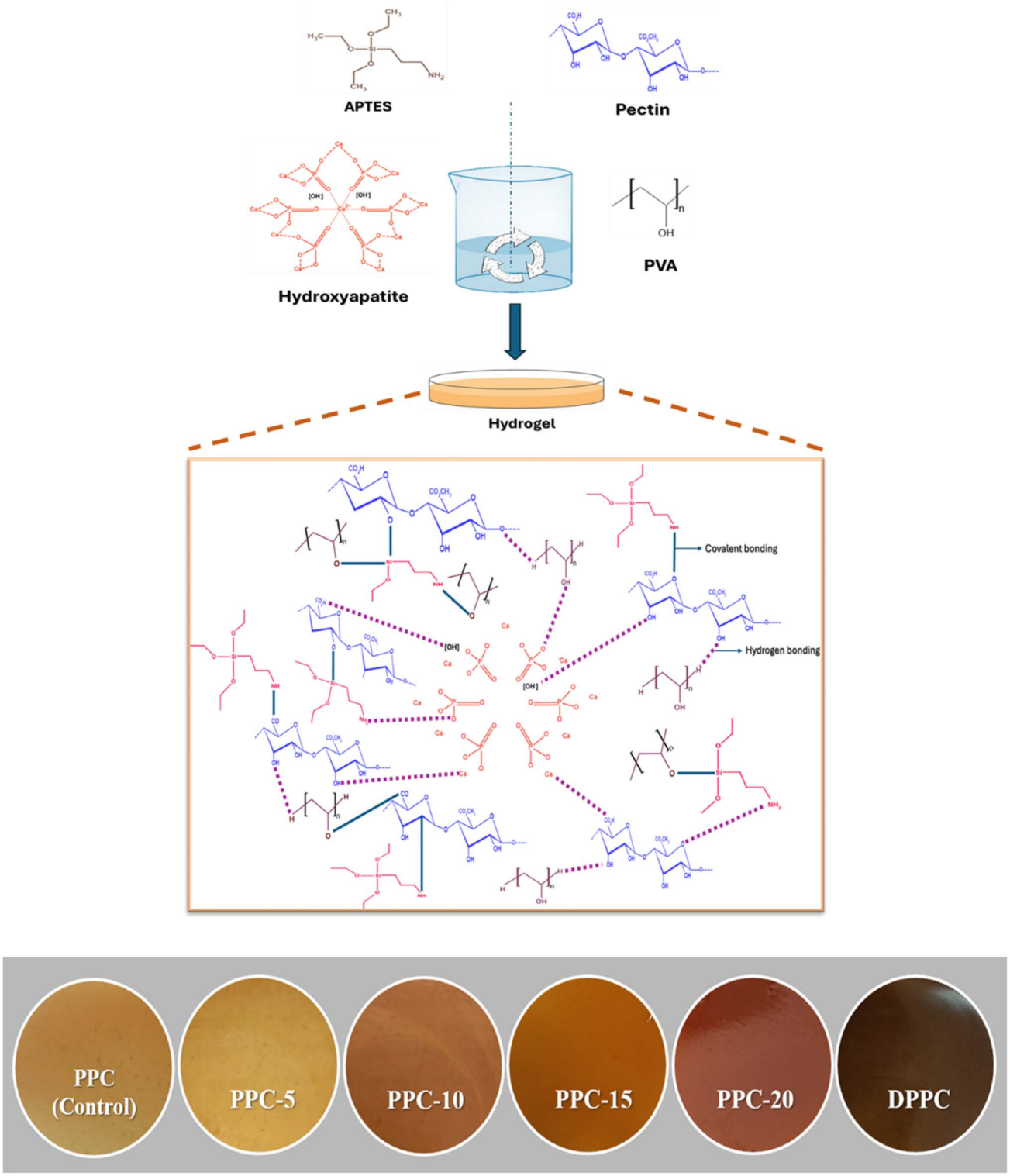

Fig. 2 The suggested scheme for the HAp-incorporated PEC/PVA/APTES/HAp hydrogel, along with the pictures of the synthesized hydrogels.

peaks of HAp, which are attributed to the phosphate and carbonate groups, were seen at 923–1024 cm^{-1} and 1418 cm^{-1}, respectively. At 1441 cm^{-1}, the C–N representative peak of the APTES was detected. The $-CH_2$ and C–O (in pectin, PVA, and APTES) were linked to bands at 1329 cm^{-1} and 1081 cm^{-1}, respectively. The presence of the functional groups of each component in the produced hydrogels is confirmed by Fig. 3(b), which displays comparable spectral peaks of all hydrogels with varying intensities depending on their composition.

Open Access Article. Published on 22 August 2025. Downloaded on 11/16/2025 4:40:19 AM.
This article is licensed under a Creative Commons Attribution-NonCommercial 3.0 Unported Licence.

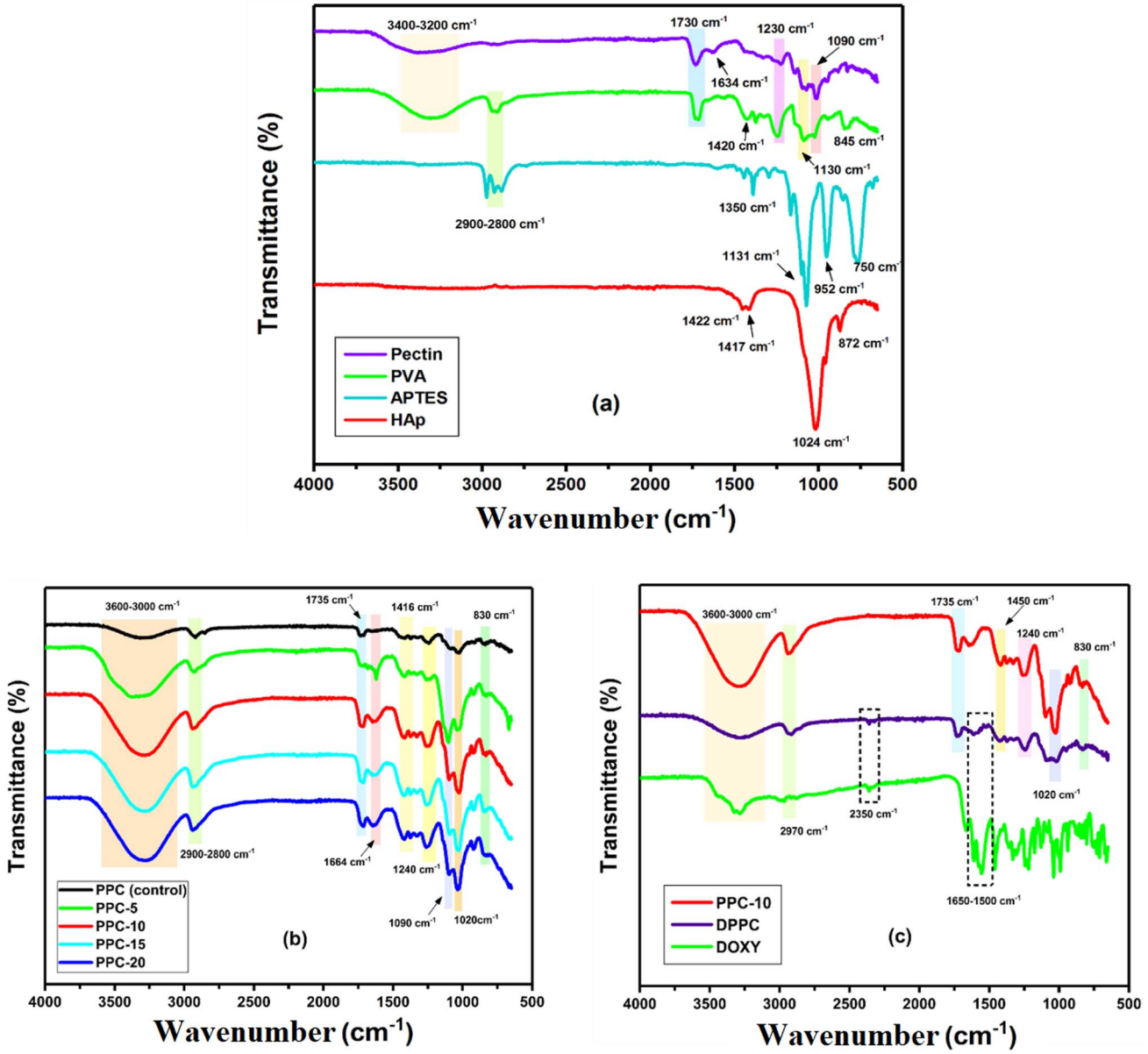

Fig. 3 FTIR spectra of the (a) pure components, (b) fabricated PPC hydrogels, and (c) pure DOXY and DOXY-loaded PPC-10 (DPPC).

However, the FTIR spectra for DOXY showed distinctive O–H and N–H stretching peaks at 3200–3500 cm^{-1}. At 2967 cm^{-1}, 1680 cm^{-1} and 1459 cm^{-1}, respectively, the C–H, C═O, and C–N stretching modes were discernible. Furthermore, the amide carbonyl stretching was seen at 1610 cm^{-1} and the peak at 1620 cm^{-1} is associated with C═O stretching in the aromatic ring.[49] No peak shift was seen in DPPC. In contrast to PPC-10, comparable peaks with lower intensity and broadness values were found. Additionally, the 1500–1650 cm^{-1} region verified the effective DOXY loading on DPPC, as shown in Fig. 3(c).

3.2.2 Thermal analysis. Thermogravimetric analysis of PPC (control), PPC-5, PPC-10, PPC-15, PPC-20 and DPPC was performed to assess the thermal stability of the hydrogels. Weight loss was observed with respect to temperature variations. The results are presented in Fig. 4(a), which show that the hydrogel stability is enhanced when the concentration of HAp filler is raised. Although the composition of each hydrogel specimen was the same, only the amounts of HAp (0–20 mg) varied. Out of all the blank hydrogels, PPC-20 (containing 20 mg HAp) had the highest stability. Because HAp contains Ca^{2+} ions, which can speed up pectin gelation and raise the cross-linking density of the polymer matrix, it improves the compactness and stabilities of the hydrogel compositions.[50] Additionally, HAp has a number of groups that are responsible for the strong hydrogen bond formation with the hydrogel matrix, which increases the hydrogel's strength and thermal stability.[51]

The TGA curves clearly showed the three-phase breakdown of the pectin skeleton. The initial stage of the breakdown occurs between 15 and 210 °C, where solvent molecules and moisture are eliminated. PVA and pectin are hydrophilic, so a significant

 © 2025 The Author(s). Published by the Royal Society of Chemistry

Open Access Article. Published on 22 August 2025. Downloaded on 11/16/2025 4:40:19 AM.
This article is licensed under a Creative Commons Attribution-NonCommercial 3.0 Unported Licence.

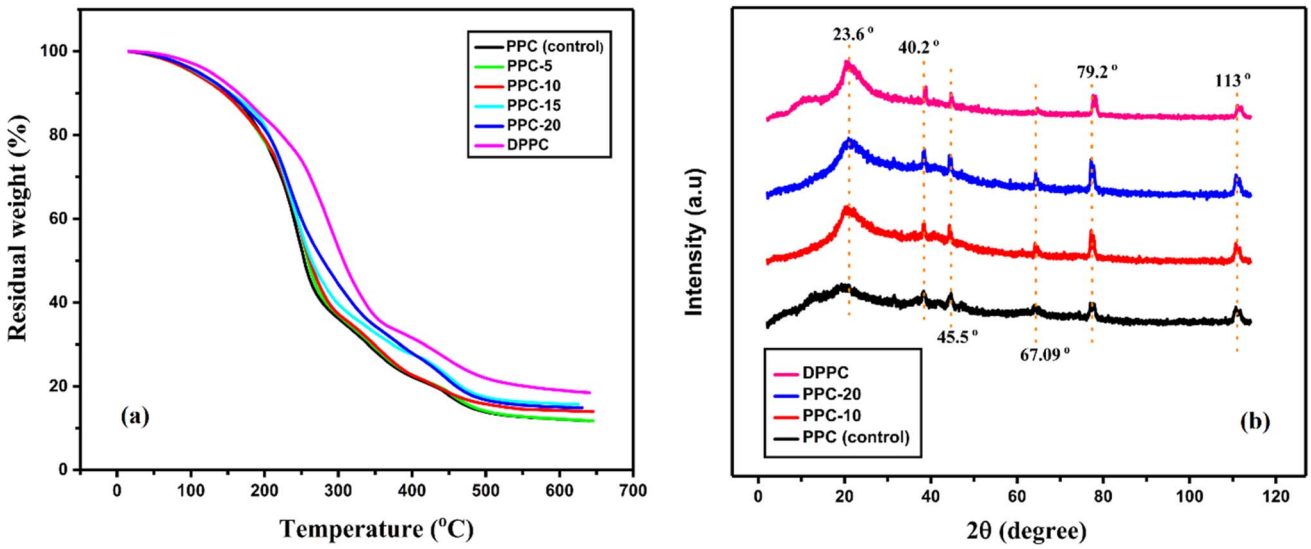

Fig. 4 (a) Thermograms and (b) X-ray diffractograms of the fabricated pectin-based PEC/PVA/APTES/HAp hydrogels.

portion of the weight loss can be due to water evaporation, especially in the early stages of the heating process. The second phase ranged from 220 to 290 °C, which is due to degradation in the side chains of polymeric skeletons. The third and final stage at 290–650 °C is attributed to the degradation in the residual polymeric backbone.[52] HAp provides thermal stability due to its strong carbon–carbon bonds, which show minimal weight loss until temperatures exceed 500 °C. APTES, due to its silane groups, also provides stability, with decomposition likely to occur at temperatures above 400 °C.[53] Furthermore, the TGA curve of the DOXY-loaded PPC-10 (DPPC) shows the significant attractive forces between the drug and hydrogel because of the hydroxyl and amide groups in DOXY that form strong hydrogen bonds with pectin, PVA, and APTES, while there are electrostatic interactions with HAp.[54] These interactions increase the cross-link density, reducing the polymer chain mobility and improving the resistance of the hydrogel to thermal degradation.[55] The residual weights of the polymers for PPC (control), PPC-5, PPC-10, PPC-15 and PPC-20, as well as DPPC, at different temperatures are displayed in Table 2.

The TGA profiles of the hydrogels reveal clear differences in thermal stability and residual weight as a function of hydroxyapatite (HAp) content and drug loading. The control hydrogel (PPC), containing 0 mg of HAp, shows the lowest thermal stability, with a final residual weight of 12.15% at 600 °C, indicating complete degradation of the organic matrix and minimal inorganic residue. As the HAp content increases from PPC-5 to PPC-20 (5 mg to 20 mg), there is a progressive rise in residual weight at higher temperatures, demonstrating the contribution of thermally stable inorganic HAp to the overall mass. This increase also reflects the improved structural robustness due to enhanced crosslinking and filler reinforcement. DPPC exhibited the highest thermal stability (Table 2), which can be attributed to the potential interactions between DOXY and the hydrogel matrix. Overall, these differences confirm that both HAp incorporation and drug loading significantly influence the thermal degradation behavior and residual mass of the hydrogel system.

Table 2 Residual weights of the hydrogels at various temperatures

	Residual weight (%)					
Hydrogels	100 °C	200 °C	300 °C	400 °C	500 °C	600 °C
PPC (control)	95.41	78.58	36.14	22.28	13.83	12.15
PPC-5	95.14	78.39	36.89	22.70	14.04	12.20
PPC-10	95.23	78.95	37.15	22.69	15.76	14.23
PPC-15	95.79	81.30	39.51	27.66	17.40	15.03
PPC-20	95.86	82.13	44.26	27.92	16.73	15.83
DPPC	97.21	84.04	52.77	31.50	21.95	19.08

3.2.3 XRD analysis. PPC (control), PPC-5, PPC-10, PPC-15, PPC-20, and DPPC underwent XRD examination; the results are displayed in Fig. 4(b). In XRD analysis, the major peaks at $2\theta = 19.2°$ to 20.1° (related to the 101 plane) and a shoulder peak at $2\theta = 22.5°$ to 22.74°, usually represent the semi-crystalline nature of PVA, while additional peaks at $2\theta = 11.2°$, 15.3°, 16.1° and 40.3° show the different aspects of the polymer's structure and hydrogen bonding.[56] In the current XRD patterns, peaks appeared within the same 2θ range, confirming the presence of PVA in all of the samples. The XRD patterns also confirmed the presence of pectin, which is in agreement with the literature. It shows peaks at 2θ values of 18.21°, 20.14°, 22.42°, 39.36°, 42.54°, 45.23°, 67.11° and 79.14°.[57] The formation of intermolecular interactions between the hydrogel components may have caused the diffraction peaks that emerged at $2\theta = 113°$.[58] A broader hump at $2\theta° = 23.6°$ in the XRD patterns represents the amorphous nature of the hydrogels, resulting from the peaks' widening and convergence in XRD. Similar amorphous interactions have been reported in the literature.[59]

All blank hydrogel specimens had the same composition and varied only in the amount of HAp (0, 10, and 20 mg).

Open Access Article. Published on 22 August 2025. Downloaded on 11/16/2025 4:40:19 AM.
This article is licensed under a Creative Commons Attribution-NonCommercial 3.0 Unported Licence.

Furthermore, the chemical cross-linking caused crystallinity, which ultimately impacted the intensity levels. PPC-20 therefore showed greater intensity values, while PPC (control) showed lower intensity values. XRD patterns suggest that all of the ingredients were successfully combined to create hydrogels with an amorphous character. The suitability of pectin for hydrogel synthesis with porous and amorphous frameworks was also shown by the XRD results, and can be further investigated for several biomedical applications like drug delivery and wound healing.

3.2.4 SEM analysis. SEM is a technique used for analyzing the surface morphology and structural features of hydrogel films. Fig. 5(a) shows the SEM images of PPC-10. The dense, compact, heterogeneous, porous and rough morphology was seen in the SEM pictures. Additionally, multi-dimensional structural spots were observed on the hydrogels' upper surface. The microstructure of the hydrogels has tiny pores that allow solvent molecules to enter and exit. Since microscopic pores assure solvent and drug retentions for a longer period, they provide sustained release. Thus, small pores are preferred for drug release in biomedical applications.[48] Fig. 5(b) presents the SEM micrograph of DPPC. The surface of DPPC is more heterogeneous, porous and multifaceted with evenly distributed DOXY molecules over the surface. SEM analysis confirmed not only effective mixing and synthesis of hydrogels, but also verified effective DOXY loading on PPC-10.[60]

3.3 *In vitro* biodegradation studies

The *in vitro* biodegradation of PEC/PVA/APTES/HAp hydrogels involves the breakdown of its constituent parts under physiological or simulated biological conditions. The presence of the biopolymer pectin is primarily responsible for the degradation in hydrogels. It has glycosidic bonds between its monomers, which the enzymes can readily break in an *in vivo* environment. As a result, it produces polysaccharides with a reduced molecular weight that can enter the metabolic pathways.[61] After adding 30 mg of each hydrogel to a freshly prepared PBS solution, the weight loss (%) was calculated after the first, third, seventh, fourteen, and twenty-one days. The biodegradation rates of PPC (control), PPC-5, PPC-10, PPC-15, and PPC-20 hydrogels in PBS were 93, 82.70, 80, 75.33, and 72.85%, respectively, as illustrated in Fig. 6(a). Likewise, as shown in Fig. 6(b), the hydrogel's biodegradation was examined in proteinase-K solution. PPC (control), PPC-5, PPC-10, PPC-15, and PPC-20 underwent 93.33%, 82%, 83.3%, 76.67%, and 73.34% biodegradation, respectively. The non-linear biodegradation of hydrogels is readily apparent with faster degradation in the beginning. Furthermore, biodegradation occurs more slowly in PBS than in proteinase-K solution. The biodegradation data are provided in the supplementary material as Tables S2 and S3.

In both PBS and enzyme solution, the biodegradation of the PEC/PVA/APTES/HAp hydrogel was negatively impacted by an increase in the HAp concentration. HAp increases compactness due to the presence of Ca^{2+} ions that can accelerate the gelation of pectin and increase the cross-linking density of the polymer matrix.[62] Moreover, HAp has several groups which can form strong hydrogen bonds within the hydrogel matrix, enhancing the strength of the hydrogels.[39]

3.4 Cell viability studies

HEK-293 cells were used to test the cell viability of the PPC (control), PPC-5, PPC-10, PPC-15 and PPC-20 hydrogels. The absorbance measurements were made after 24 h, and the results of MTT assay were compared using HEK-293 cells as a reference (Fig. 6(c)). The MTT experimental findings

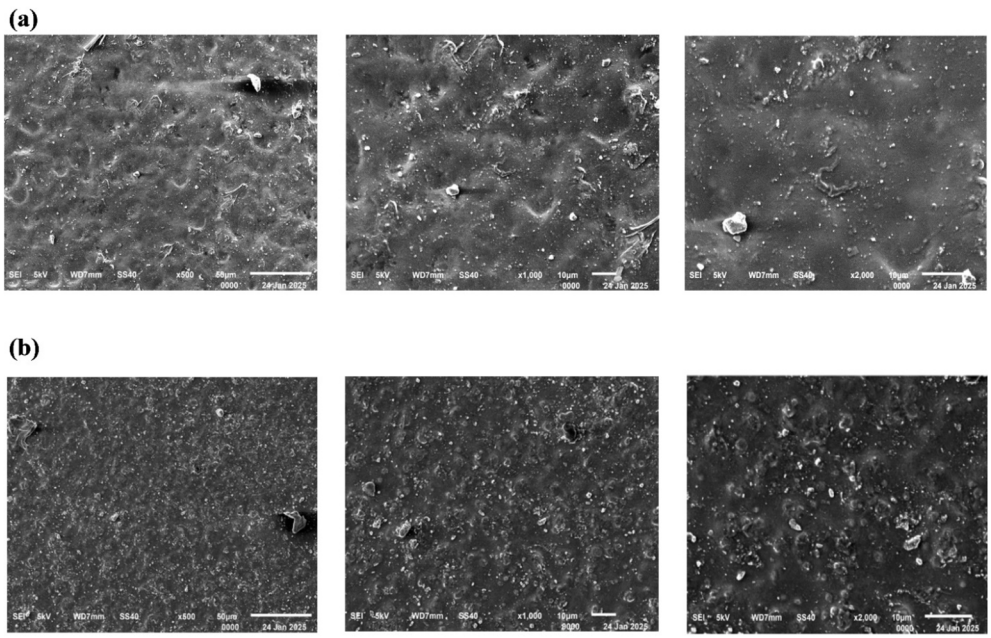

Fig. 5 (a) SEM micrographs of PPC-10 at various magnifications, (b) SEM micrographs of DPPC (DOXY-loaded PPC-10).

 © 2025 The Author(s). Published by the Royal Society of Chemistry

Open Access Article. Published on 22 August 2025. Downloaded on 11/16/2025 4:40:19 AM.
This article is licensed under a Creative Commons Attribution-NonCommercial 3.0 Unported Licence.

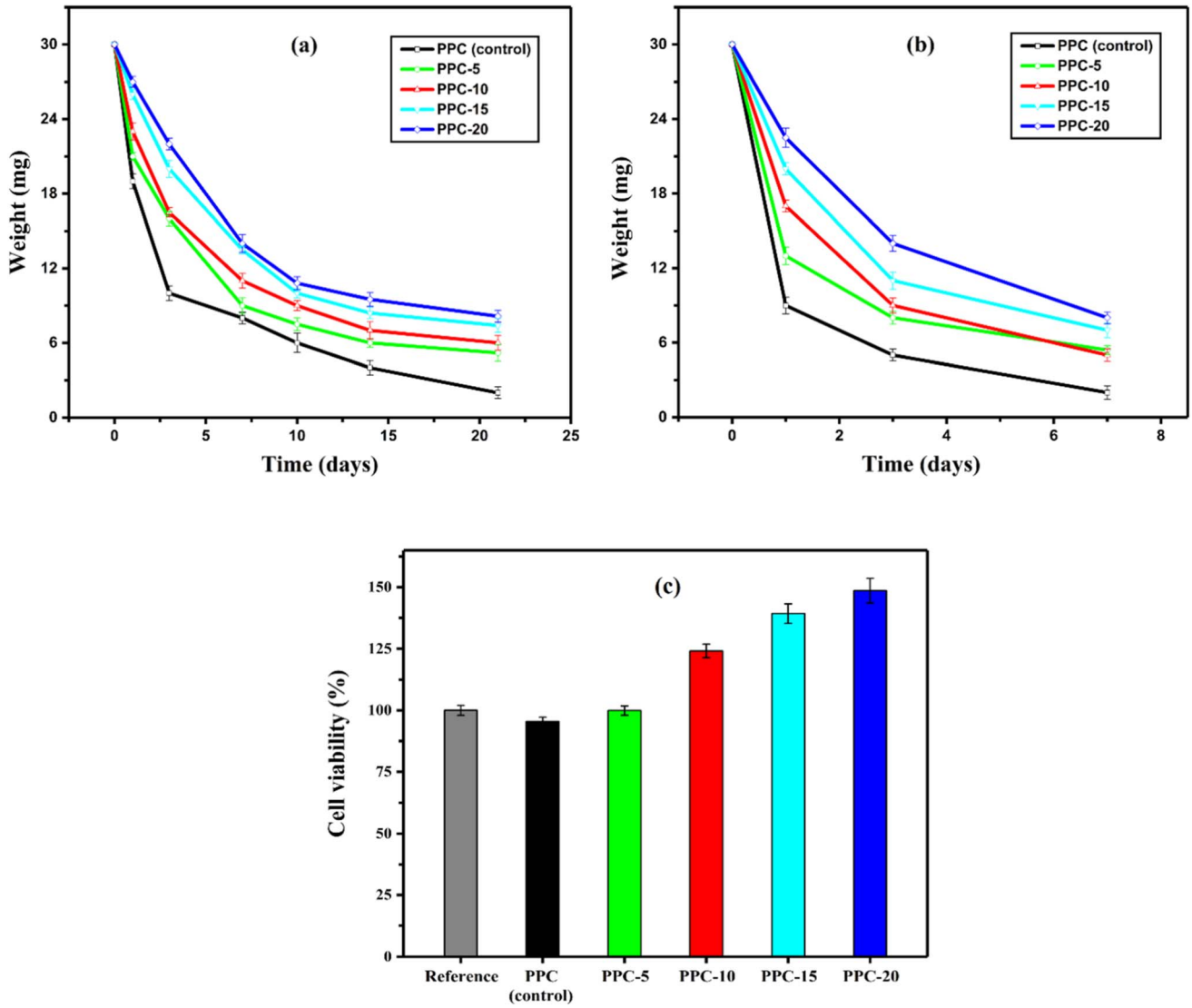

Fig. 6 (a) Biodegradation studies of hydrogels in (a) PBS and in (b) proteinase-K. (c) Cell viability of the hydrogels.

demonstrated that cells were able to go through a cell cycle and multiply (Fig. S1–S6 in SI). The rise in the HAp amount increased this propensity by creating an environment that was favorable for cell proliferation. It enhances biocompatibility and tissue integration through its osteoconductive and bioactive qualities, which promote cell attachment, proliferation and differentiation.[63] All hydrogels showed increased cell proliferation as compared to the reference group. This indicated that the hydrogels were suitable for a variety of medico-biological uses, including wound dressings, tissue engineering and drug administration. Table 3 provides the statistical parameters computed from the cell line results.

Table 3 The fabricated hydrogel's statistical parameters for cell viability

	Statistical parameters					
Samples	*N*	Average	SD	Sum	Median	Cell viability (%)
Reference	3	1.5848	0.0878	6.3391	1.6005	100
PPC (control)	3	1.5171	0.0793	4.5512	1.4968	95.73
PPC-5	3	1.5092	0.0803	4.5277	1.4802	95.23
PPC-10	3	1.8745	0.2465	5.6234	1.7462	118.28
PPC-15	3	2.1030	0.4677	6.3091	1.8625	132.70
PPC-20	3	2.2434	0.5701	6.7303	1.9385	141.56

3.5 Swelling studies

3.5.1 Swelling in DW. Hydrogels can absorb solvents at thousands of times their dry weight due to their hydrophilic nature. The special ability of hydrogels to mimic living tissues makes them a potentially useful substance for biological purposes.[64] Therefore, DW was used to evaluate the synthesized hydrogels' capacity to swell. Fig. 7(a) displays these findings. Pectin's hydrophilic groups connect with water molecules *via* electrostatic and hydrogen bonding interactions, which allows it to absorb and hold a lot of water.[44] Pectin hydrogels therefore

Open Access Article. Published on 22 August 2025. Downloaded on 11/16/2025 4:40:19 AM.
This article is licensed under a Creative Commons Attribution-NonCommercial 3.0 Unported Licence.

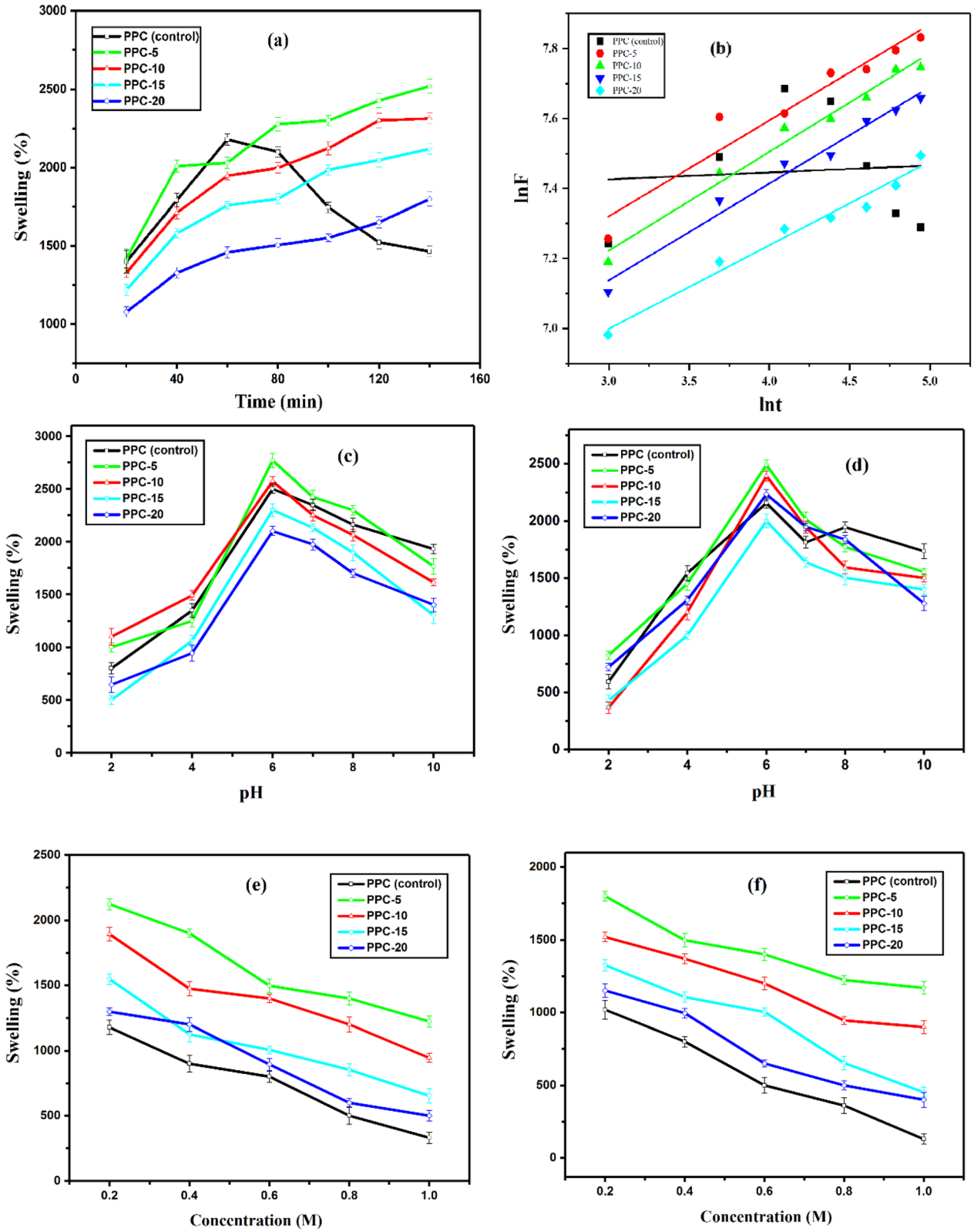

Fig. 7 (a) Swelling pattern of the hydrogels in DW. (b) Calibration curves for the determination of diffusion parameters in DW swelling. The hydrogels' swelling at different pH values in (c) non-buffer and (d) buffer solutions. The swelling of the hydrogels in electrolyte solutions containing (e) NaCl and (f) $CaCl_2$.

 © 2025 The Author(s). Published by the Royal Society of Chemistry

Open Access Article. Published on 22 August 2025. Downloaded on 11/16/2025 4:40:19 AM.
This article is licensed under a Creative Commons Attribution-NonCommercial 3.0 Unported Licence.

showed favorable swelling patterns. PPC-5 displays the highest swelling capability (2519%). Due to the lack of filler that stabilized other hydrogels in aqueous media, PPC (control) showed an early increase in swelling volumes (2179%), followed by a steady reduction. The swelling capability of hydrogels decreases with an increase in the concentration of HAp because it enhances the hydrogel compactness by forming strong ionic and hydrogen bonds with the polymer functional groups, strengthening the structure, reducing the porosity, and improving the mechanical robustness.[65]

After 140 min, the swelling equilibrium was reached. All of the hydrogels, except for PPC (control), showed a linear rise in the swelling percentage with time, and the variation was found to be slight. Therefore, the addition of HAp gave stability to the hydrogel films. Eqn (4) is used to determine the kind of diffusion mechanism that causes the swelling of the hydrogel. A graph of "ln F" *vs.* "ln T" is plotted and is demonstrated in Fig. 7(b), and the calculated diffusion parameters are provided in Table 4. The diffusion process followed Fick's law because the values of n for PPC (control), PPC-5, PPC-10, PPC-15 and PPC-20 are less than 0.5.[66–68]

3.5.2 Swelling in non-buffer and buffer solutions. The nature of the medium, the ionic concentration and the proportion of bases and acids all affect the swelling of hydrogels.[69] The hydrogels' capacity to swell, in both the non-buffer and buffer solutions at varying pH values, is demonstrated in Fig. 7(c) and (d), respectively. At pH 6, the hydrogels exhibited their highest swelling. In buffers and non-buffers, PPC-5 had the highest swelling volumes of 2490% and 2767%, respectively. Pectin hydrogels generally show greater swelling at basic pH due to the deprotonation of functional groups, resulting in greater electrostatic repulsion and osmotic pressure, which enhances swelling.[70] However, HAp-incorporated pectin hydrogels showed maximum swelling at pH 6. Calcium ions in HAp reduce hydrogel swelling at higher pH by forming ionic cross-links with negatively charged groups in the polymer, stabilizing the network and limiting water uptake.[65] They neutralize electrostatic repulsion and increase network rigidity, resulting in a more compact hydrogel structure with lower swelling capacity.[37]

The HAp amount inversely affected the hydrogel swelling because of its ability to form strong attractive forces with various functionalities in pectin, APTES and PVA.[71] In non-buffers, PPC (control), PPC-5, PPC-10, PPC-15, and PPC-20 showed swelling of 2500%, 2767%, 2571%, 2300%, and 2100% at pH 6, respectively. PPC (control), PPC-5, PPC-10, PPC-15, and PPC-20 demonstrated 2156%, 2490%, 2392%, 2000% and 2233% swelling in buffers, respectively. The pattern of hydrogel swelling is the same in the buffer and non-buffer solutions. However, swelling is much more pronounced in the non-buffer solutions. This is because the non-buffers are made only with NaOH and HCl, so there are less positive and negative ions in them as compared to buffer solutions.[72] This increases the osmotic pressure and water uptake by the hydrogels. In medical-biological applications, these hydrogels' distinct and pH-dependent swelling properties can be utilized for drug release. The swelling percentage data of hydrogels in DW, buffer, and non-buffer solutions are provided in the supplementary material (Table S4).

3.5.3 Swelling in ionic solutions. The primary determinants of swelling behavior in an electrolyte solution are ionic sizes and charge density.[73] Thus, as shown in Fig. 7(e) and (f), the swelling behavior of hydrogels in solutions with different concentrations of NaCl and $CaCl_2$ was investigated. The cations in these electrolytic differ, but the anion is the same. Since Na^{+1} and Ca^{+2} have distinct charge-to-size ratios, swelling volumes were reduced with the increase in the ionic charge. Compared to NaCl, the ions in the $CaCl_2$ aqueous solution are more abundant. The rise in the number of ions reduced the swelling of hydrogels.[17] In $CaCl_2$, the hydrogels displayed decreased swelling volumes. However, in NaCl, they displayed enhanced swelling volumes. Additionally, higher ionic concentrations and charge densities promote inter-chain complexation within the hydrogel matrix, preventing solvent molecules from entering and producing a compact hydrogel.[74]

Table 4 The calculated diffusion parameters for the swelling of hydrogels

	Hydrogel samples				
Parameters	PPC (control)	PPC-5	PPC-10	PPC-15	PPC-20
Adj. R-square	−0.193	0.920	0.975	0.975	0.968
R-square (COD)	0.006	0.933	0.980	0.980	0.974
Slope (n)	0.020	0.274	0.282	0.277	0.239
Intercept	7.367	6.497	6.376	6.308	6.282
k	1582.88	663.15	587.57	548.95	534.86

3.6 Antibacterial studies

Fig. 8(a) and (b) show the antibacterial activity of the PPC (control), PPC-5, PPC-10, PPC-15, and PPC-20 hydrogels against *E. coli* and *S. aureus*, respectively. PPC-5 exhibited greater bactericidal activity against both *S. aureus* and *E. coli*, with I_z values of 3.8 ± 0.02 mm and 8 ± 0.04 mm, respectively (Table 5). Comparatively low I_z values for other HAp-reinforced hydrogels could be linked to its stronger binding when incorporated in the hydrogel's network in greater amounts; hence, resulting in decreased antibacterial activity.[65] Pectin is the major antibacterial agent, and the decrease in antibacterial activity with increasing HAp concentration can be attributed to physical and structural changes in the hydrogel matrix. At higher HAp concentrations, the hydrogel network became more compact or rigid, resulting in a reduced ability for the hydrogel to swell or expand, which limits the pectin ability to interact with bacteria. Furthermore, the increased concentration of HAp may alter the surface charge or topography of the hydrogel, which could influence bacterial adhesion or growth. Overall, the antibacterial efficiency of all hydrogels was found to be superior for Gram-negative (*E. coli*) bacteria than for Gram positive (*S. aureus*) bacteria. Each hydrogel specimen's I_z value is provided in Table 5.

Open Access Article. Published on 22 August 2025. Downloaded on 11/16/2025 4:40:19 AM.
This article is licensed under a Creative Commons Attribution-NonCommercial 3.0 Unported Licence.

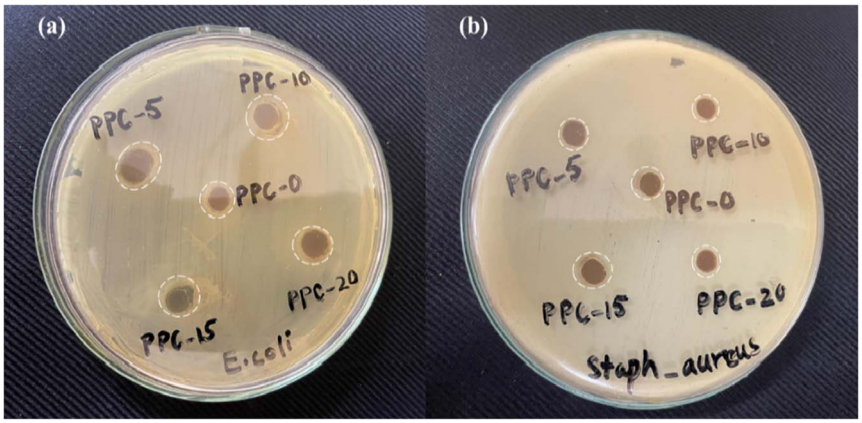

Fig. 8 Antibacterial activity test of the hydrogels against (a) *E. coli* and (b) *S. aureus*.

Table 5 I_z values of the hydrogels against *E. coli* and *S. aureus*, along with mean ± SD

	I_z (mm)				
Bacteria	PPC (control)	PPC-5	PPC-10	PPC-15	PPC-20
E. coli	3 ± 0.02	8 ± 0.04	5 ± 0.04	5.5 ± 0.02	6 ± 0.02
S. aureus	2.3 ± 0.03	3.8 ± 0.02	2.8 ± 0.07	3 ± 0.01	2 ± 0.04

3.7 *In vitro* drug (DOXY) release studies

Drug release from the hydrogel matrix is primarily influenced by swelling behavior, and the formation of intermolecular interactions between the polar functionalities of the hydrogel and drug.[75] In this context, PPC-10 was loaded with 50 mg of DOXY because of its favorable swelling response, stability, and cell survival. The code for the DOXY-loaded PPC-10 hydrogel was given as DPPC. Using PBS solution, the time-dependent *in vitro* drug release was evaluated through absorption studies. Fig. 9(a) shows the standard calibration curve for DOXY, and Fig. 9(b) presents the results of the drug's linear release pattern from the hydrogel in relation to time. 88.57% of DOXY was released in 3.5 h.

The sustained release of DOXY is evident from the *in vitro* drug release patterns. Three main processes that regulate drug release from hydrogels are swelling, diffusion and erosion.[76] For drug delivery applications, researchers have documented DOXY release from a variety of biopolymeric hydrogel matrices. Kavish *et al.* synthesized glutaraldehyde-crosslinked chitosan hydrogel, which demonstrated 58% DOXY release in under 2 h.[77] In another study, collagen and hyaluronic acid-based biohybrid hydrogel membranes released 90% DOXY at pH 7.4 and 80% at pH 8.3 in 12 h, showcasing a significant drug release capability that is influenced by pH levels.[78] The 88.57% release of DOXY from PEC/PVA/APTES/HAp at pH 7.4 in 3.5 h in current studies was found to be more pronounced than that reported for its release from other biopolymeric hydrogels. The greater and sustained drug release profile is attributed to its effectiveness for use in biomedical applications, especially as a drug delivery system for treating bacterial infections of the skin, gastrointestinal system, and urinary tract, *etc.*

To verify the transport mechanism of DOXY from DPPG, the drug release numerical data were fitted into kinetic models using eqn (5)–(7) and the resulting graphs are shown in Fig. 9(c)–(e), while the relevant data are provided in the supplementary material as Table S5. These equations explain the zero-order, Korsmeyer-Peppas, and Higuchi kinetic models, respectively, which are used to confirm the drug release mechanism.[79] The calculated parameters for these kinetic models are shown in Fig. 9(c–e, inset Tables). The regulated release of DOXY from the hydrogel was validated by the slope (0.0041, 7.837, and 0.7487) and regression R^2 (0.912, 0.966, and 0.972) values derived from the linear graphs of the zero-order, Higuchi kinetic, and Korsmeyer-Peppas models, respectively. Furthermore, they demonstrated that the time-dependent diffusion-controlled mechanism governs the release of drugs from the hydrogel.[58] All of the hydrogels without drug followed Fickian diffusion, as obvious from the slope ($n < 0.5$) values in Table 4. However, release of the drug (DOXY) from the hydrogel *via* examining the kinetic models revealed that Fickian diffusion was only followed in the zero-order kinetic model, where the slope value was found to be lesser than 0.5. On the other hand, anomalous diffusion occurred in the other two models due to the greater slope values.[67,68] However, the numerical value of the slope was found in accordance with the $n > 1$ and $0.45 < n > 0.89$ for the Higuchi and Korsmeyer-Peppas models, respectively, indicating that the anomalous diffusion process was involved in DOXY release from APTES cross-linked Pectin/PVA/Hap hydrogels *via* Super Case and non-Fickian diffusion, respectively.[67,80] It is evident from the regression coefficients that the drug release data were best fitted to the Korsmeyer-Peppas model with greater R^2 (0.972) among all models. Therefore, DOXY release from the reported hydrogels is due to the combination of diffusion and swelling imparted by the polymeric chain relaxations in aqueous media. This is in strong agreement to the previously reported DOXY release studies.[81] In conclusion, DOXY release from the aforementioned pectin-based gels obeyed the non-Fickian release mechanism. Initially, the drug was released due to the swelling, which is relatively faster. Later on, DOXY concentration gradient regulated its release *via* diffusion process.

 © 2025 The Author(s). Published by the Royal Society of Chemistry

Open Access Article. Published on 22 August 2025. Downloaded on 11/16/2025 4:40:19 AM.
This article is licensed under a Creative Commons Attribution-NonCommercial 3.0 Unported Licence.

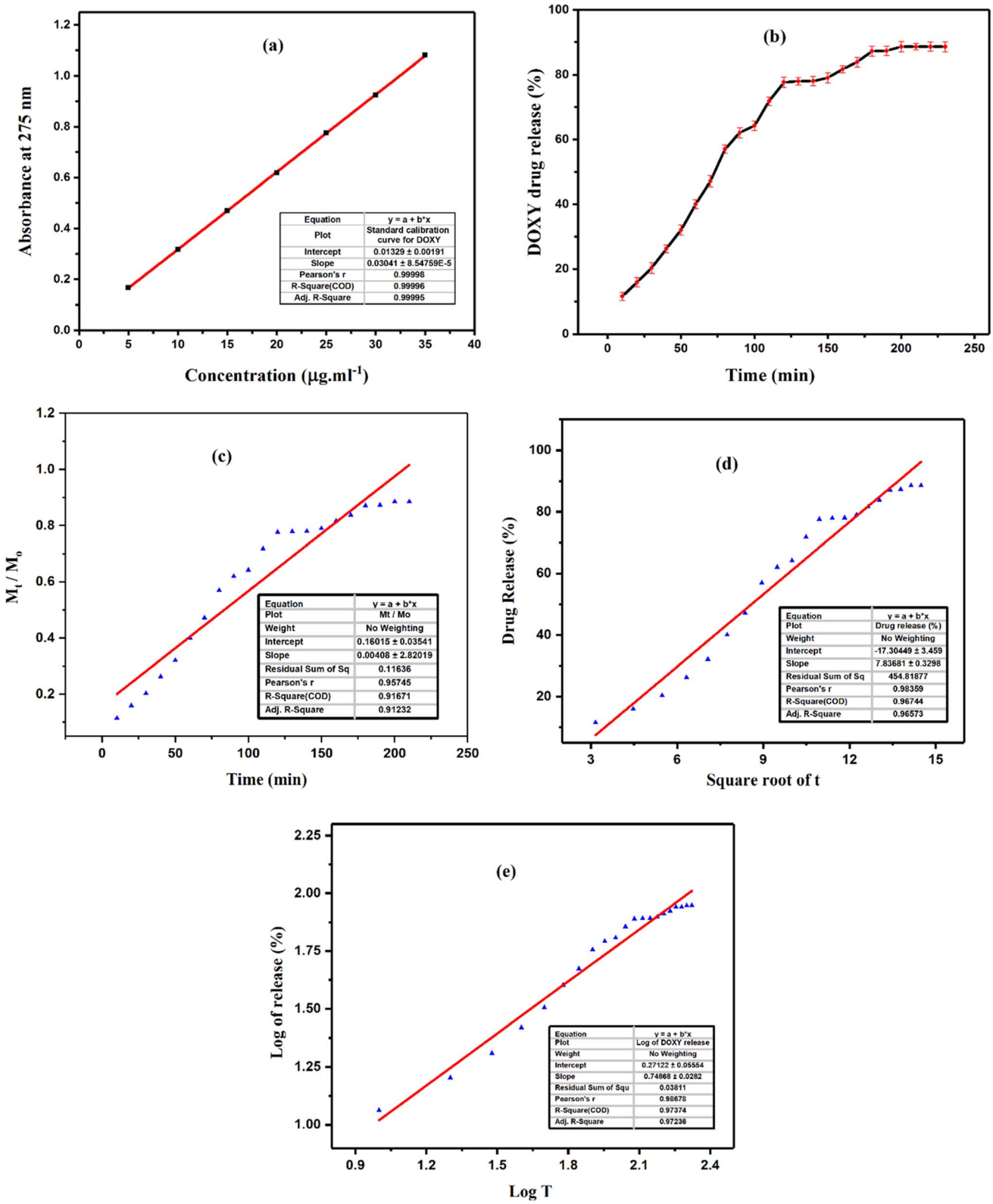

Fig. 9 (a) Standard calibration curve for DOXY, (b) *in vitro* DOXY release in PBS, (c) zero-order kinetic model, (d) Higuchi model, (e) Korsmeyer-Peppas model, inset tables in (c–e) for kinetic parameters.

3.8 *In vivo* wound healing studies

The wound healing process is dynamic and usually progresses from the first inflammatory response to full resolution, and ultimately healing.[82] Hydrogel-based wound dressing development from biomaterials has garnered much research attention since hydrogels appear to be favorable media for promoting

Open Access Article. Published on 22 August 2025. Downloaded on 11/16/2025 4:40:19 AM.
This article is licensed under a Creative Commons Attribution-NonCommercial 3.0 Unported Licence.

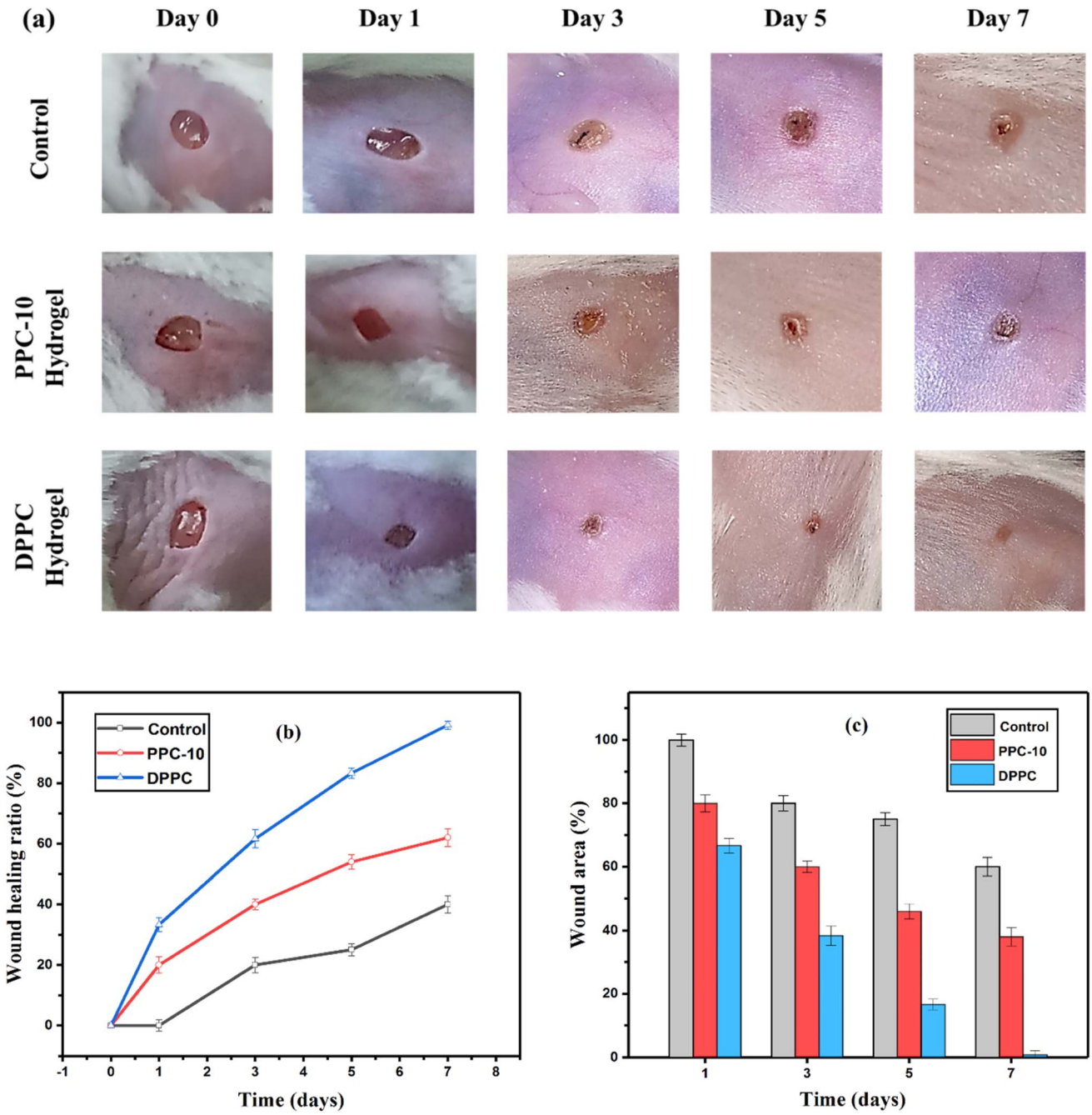

Fig. 10 (a) Representative images of the wounds treated with the PPC series over an interval of 7 days, (b) wound healing ratio with respect to time, and (c) quantification of wound contraction during the healing process.

wound healing due to their high water content and capacity for water retention.[83] An animal experiment was conducted in this study to evaluate the hydrogel's efficacy in the healing of skin wounds. Fig. 10(a) shows the representative images of the wounds' sizes treated with PPC series during the monitoring of the wound healing process (day 1–day 7). Additionally, to quantitatively assess the wound healing process, the decrease in the wound size was computed using eqn (8) and is displayed in Fig. 10(b) and (c). There were signs of infection and inflammation, as well as a comparatively slower healing process in the control group, with daily pyodine applications.

Comparing the PPC-10 and DPPC hydrogel treatment groups to the control group, the hydrogel groups exhibited better healing and no signs of infection. At all time points, the DPPC-treated wounds showed significantly greater wound healing than the PPC-10 treated wounds. This could be attributed to the role of HAp in enhancing the binding affinity between the drug and the inorganic phase and may reduce porosity, leading to a slower and more sustained release of DOXY. This prolonged release supports wound healing over an extended period by maintaining effective drug concentrations and leveraging HAp's regenerative properties.

 © 2025 The Author(s). Published by the Royal Society of Chemistry

Open Access Article. Published on 22 August 2025. Downloaded on 11/16/2025 4:40:19 AM.
This article is licensed under a Creative Commons Attribution-NonCommercial 3.0 Unported Licence.

The results showed that on the third day, the group with the DPPC hydrogel dressing showed 55–61% healing, whereas the control and PPC-10 hydrogel groups showed 19–22% and 33–40% healing, respectively. According to earlier research, the hydrogel dressing's ability to heal over 50% of the wound in 14 days suggests that the dressing was well developed.[54] Furthermore, on the seventh day, the DPPC hydrogel group's wound healing rate was 99.17%, greater than that of other groups, demonstrating the effective drug release from the hydrogel and the skin regenerative properties of the synthesized hydrogels. A complete healing of 5–6 mm excision wound was observed in 8 days in the case of DPPC. Rezvanian *et al.* produced a simvastatin-loaded alginate-pectin hydrogel film, and documented the percent closure of wound during a period of 21 days of treatment.[84] In another study, a chitosan-containing hydrogel improved wound healing by 99.3 ± 0.5%, whereas the control group improved by 90 ± 0.0% in 27 days. However, observations did not indicate any improvement up to the 7th day of the experiment.[85]

4. Conclusions

Structural and mechanical improvements by cross-linkers and fillers in multifunctional hydrogels have made them viable materials for various biomedical applications. This study aims to develop novel pH-sensitive PEC/PVA/APTES/HAp hydrogels, and to investigate them for applications requiring prolonged DOXY release. By varying the amount of HAp, novel PEC/PVA/APTES/HAp pH-sensitive hydrogels were synthesized and tested for applications requiring prolonged DOXY release. According to the FTIR data, there was a well-defined binding between the functional groups linked to Pectin, PVA, APTES, and HAp. SEM, XRD and TGA confirmed the porosity, amorphous nature and thermal stability of the hydrogels. The hydrogels' incorporation of HAp is closely linked to their thermal and bio-degradational stabilities. Because PPC-20 contained the highest concentration of filler, it was the most stable of the hydrogels. By measuring the proportion of swelling in non-buffer and buffer solutions, the hydrogel's sensitivity to pH was demonstrated. Each hydrogel showed the highest percentage of swelling at pH 6. However, because of polymeric complexation, the increase in the electrolyte's concentration decreased the swelling percentage. The sustained release of DOXY in PBS was evaluated *in vitro*, and it was found to be 88.57% in 3.5 h. The DOXY release from the DPPC hydrogel preferably followed the Korsmeyer-Peppas model. In the wound healing *in vivo* studies, the hydrogels showed exceptional performance by showing ∼100% healing of 6 mm excision wounds in 8 days. The efficacy of HAp-incorporated PEC/PVA/APTES/HAp hydrogels makes them an effective, cytocompatible, bio-degradable, pH-responsive and antibacterial platform that can be used for various biomedical applications.

Author contributions

Hirra Manzoor: data curation, investigation, formal analysis, software, writing—original draft, writing—review & editing. Nasima Arshad: conceptualization, project administration, supervision, methodology, visualization, validation, resources, writing—original draft, writing—review & editing. Muhammad A. U. R. Qureshi: methodology, validation, formal analysis. Aneela Javed: methodology.

Conflicts of interest

There are no conflicts to declare.

Data availability

The data supporting this article have been included in the experimental part and as part of the SI.

Fig. S1–S6 and Tables S1–S5. See DOI: https://doi.org/10.1039/d5ra01989c.

Abbreviations

3D	Three-dimensional
APTES	Aminopropyltriethoxysilane
DOXY	Doxycycline
DW *E. coli*	Distilled water *Escherichia coli*
FTIR	Fourier transform infrared spectroscopy
Hap	Hydroxyapatite
HEK	Human embryonic kidney
I_z LB	Inhibition zone Lysogeny broth
MTT	(3-[4,5-Dimethylthiazol-2-yl]-2,5 diphenyl tetrazolium bromide)
NIH	National Institute of Health
PBS PEC	Phosphate buffer saline pectin
PVA	Poly(vinyl alcohol)
SD	Standard deviation
SEM *S. aureus*	Scanning electron microscopy *Staphylococcus aureus*
TGA	Thermogravimetric analysis
XRD	X-ray diffraction

Acknowledgements

The laboratory facilities at Allama Iqbal Open University, where this research was conducted, are gratefully acknowledged. We also extend our gratitude to Mr Rahim Shah, Chief BPD, NIH, Islamabad, for *in vivo* work facilitation under the assistance of Dr Hussain (VMD).

References

1 B. Liu and K. Chen, Advances in hydrogel-based drug delivery systems, *Gels*, 2024, **10**(4), 262, DOI: 10.3390/gels10040262.
2 N. Kasmi, L. Pieruccioni, E. Pitot, I. Fourquaux, A. Wodrinski, L. Gibot and J. Fitremann, The potential of carbohydrate supramolecular hydrogels for long-term 3D culture of primary fibroblasts, *J. Mater. Chem. B*, 2025, **13**, 4386–4405, DOI: 10.1039/D4TB02658F.

Open Access Article. Published on 22 August 2025. Downloaded on 11/16/2025 4:40:19 AM.
This article is licensed under a Creative Commons Attribution-NonCommercial 3.0 Unported Licence.

3 K. V. G. Sinad, R. C. Ebubechukwu and C. K. Chu, Recent advances in double network hydrogels based on naturally-derived polymers: synthesis, properties, and biological applications, *J. Mater. Chem. B*, 2023, **11**(48), 11460–11482, DOI: 10.1039/D3TB00773A.
4 S. Bashir, M. Hina, J. Iqbal, A. H. Rajpar, M. A. Mujtaba, N. A. Alghamdi, S. Wageh, K. Ramesh and S. Ramesh, Fundamental concepts of hydrogels: synthesis, properties, and their applications, *Polymers*, 2022, **12**(11), 2702, DOI: 10.3390/polym12112702.
5 M. Bustamante-Torres, D. Romero-Fierro, B. Arcentales-Vera, K. Palomino, H. Magaña and E. Bucio, Hydrogels classification according to the physical or chemical interactions and as stimuli-sensitive materials, *Gels*, 2021, **7**(4), 182, DOI: 10.3390/gels7040182.
6 T. C. Ho, C. C. Chang, H. P. Chan, T. W. Chung, C. W. Shu, K. P. Chuang, T. H. Duh, M. H. Yang and Y. C. Tyan, Hydrogels: properties and applications in biomedicine, *Molecules*, 2022, **27**(9), 2902, DOI: 10.3390/molecules27092902.
7 H. K. Pradeep, D. H. Patel, M. Laxmi, C. C. Pratiksha, G. Bolakatti, P. K. GM and A. Sapre, Pharmaceutical hydrogels: a comprehensive review, *RGUHS J. Pharm. Sci.*, 2024, **14**(2), 2, DOI: 10.26463/rjps.14_2_7.
8 Y. Wang, J. Li, M. Tang, C. Peng, G. Wang, J. Wang, X. Wang, X. Chang, J. Guo and S. Gui, Smart stimuli-responsive hydrogels for drug delivery in periodontitis treatment, *Biomed. Pharmacother.*, 2023, **162**, 114688, DOI: 10.1016/j.biopha.2023.114688.
9 X. Sun, F. Yao and J. Li, Nanocomposite hydrogel-based strain and pressure sensors: a review, *J. Mater. Chem. A*, 2020, **8**(36), 18605–18623, DOI: 10.1039/D0TA06965E.
10 X. Fu, L. Hosta-Rigau, R. Chandrawati and J. Cui, Multi-stimuli-responsive polymer particles, films, and hydrogels for drug delivery, *Chem*, 2018, **4**(9), 2084–2107, DOI: 10.1016/j.chempr.2018.07.002.
11 B. Kaczmarek, K. Nadolna and A. Owczarek, Chapter-6: the physical and chemical properties of hydrogels based on natural polymers, *Hydrogels Based Nat. Polym.*, 2020, 151–172, DOI: 10.1016/B978-0-12-816421-1.00006-9.
12 R. Ahmad, O. S. Wolfbeis, Y. B. Hahn, H. N. Alshareef, L. Torsi and K. N. Salama, Deposition of nanomaterials: a crucial step in biosensor fabrication, *Mater. Today Commun.*, 2018, **17**, 289–321, DOI: 10.1016/j.mtcomm.2018.09.024.
13 J. W. Meisel and G. W. Gokel, A simplified direct lipid mixing lipoplex preparation: comparison of liposomal-, dimethylsulfoxide-, and ethanol-based methods, *Sci. Rep.*, 2016, **6**(1), 27662, DOI: 10.1038/srep27662.
14 N. Raghav, C. Vashisth, N. Mor, P. Arya, M. R. Sharma, R. Kaur, S. P. Bhatti and J. F. Kennedy, Recent advances in cellulose, pectin, carrageenan and alginate-based oral drug delivery systems, *Int. J. Biol. Macromol.*, 2023, **244**, 125357, DOI: 10.1016/j.ijbiomac.2023.125357.
15 S. Ahmad, M. Ahmad, K. Manzoor, R. Purwar and S. Ikram, A review on latest innovations in natural gums based hydrogels: preparations & applications, *Int. J. Biol. Macromol.*, 2019, **136**, 870–890, DOI: 10.1016/j.ijbiomac.2019.06.113.
16 A. K. Tamo, Nanocellulose-based hydrogels as versatile materials with interesting functional properties for tissue engineering applications, *J. Mater. Chem. A*, 2024, **12**, 7692, DOI: 10.1039/d4tb00397g.
17 H. Chamkouri, A review of hydrogels, their properties and applications in medicine, *Am. J. Biomed. Sci. Res.*, 2021, **11**(6), 485–493, DOI: 10.34297/AJBSR.2021.11.001682.
18 S. S. Ferreira, C. P. Passos, P. Madureira, M. Vilanova and M. A. Coimbra, Structure–function relationships of immunostimulatory polysaccharides: a review, *Carbohydr. Polym.*, 2015, **132**, 378–396, DOI: 10.1016/j.carbpol.2015.05.079.
19 F. Naqash, F. A. Masoodi, S. A. Rather, S. M. Wani and A. Gani, Emerging concepts in the nutraceutical and functional properties of pectin—A review, *Carbohydr. Polym.*, 2020, **168**, 227–239, DOI: 10.1016/j.carbpol.2017.03.058.
20 I. L. G. Lekhuleni, T. E. Kgatla, M. E. Mashau and A. I. O. Jideani, Physicochemical properties of South African prickly pear fruit and peel: extraction and characterisation of pectin from the peel, *Open Agric.*, 2021, **6**(1), 178–191, DOI: 10.1515/opag-2021-0216.
21 S. J. Marathe, S. B. Jadhav, S. B. Bankar, K. Kumari Dubey and R. S. Singhal, Improvements in the extraction of bioactive compounds by enzymes, *Curr. Opin. Food Sci.*, 2019, **25**, 62–72, DOI: 10.1016/j.cofs.2019.02.009.
22 R. Bharti, S. Pal, N. Prasad, Y. Kumar, B. Joseph, H. Sharma and G. K. Sahu, A comprehensive review on hydrogel, *Acta Sci. Pharm. Sci.*, 2024, **8**(6), 64–75, DOI: 10.31080/ASPS.2024.08.1070.
23 F. V. Vityazev, M. I. Fedyuneva, V. V. Golovchenko, O. A. Patova, E. U. Ipatova, E. A. Durnev, E. A. Martinson and S. G. Litvinets, Pectin-silica gels as matrices for controlled drug release in gastrointestinal tract, *Carbohydr. Polym.*, 2017, **157**, 9–20, DOI: 10.1016/j.carbpol.2016.09.048.
24 R. Awasthi, G. T. Kulkarni, M. V. Ramana, T. Jesus Andreoli Pinto, I. S. Kikuchi, D. D. Molim Ghisleni, M. Souza Braga, P. De Bank and K. Dua, Dual crosslinked pectin–alginate network as sustained release hydrophilic matrix for repaglinide, *Int. J. Biol. Macromol.*, 2017, **97**, 721–732, DOI: 10.1016/j.ijbiomac.2017.01.050.
25 L. Neufeld, H. Bianco-Peled and H. Pectin, chitosan physical hydrogels as potential drug delivery vehicles, *Int. J. Biol. Macromol.*, 2017, **101**, 852–861, DOI: 10.1016/j.ijbiomac.2017.03.167.
26 S. Thakur, J. Chaudhary, V. Kumar and V. K. Thakur, Progress in pectin based hydrogels for water purification: trends and challenges, *J. Environ. Manage.*, 2019, **238**, 210–223, DOI: 10.1016/j.jenvman.2019.03.002.
27 J. Long, A. E. Etxeberria, A. V. Nand, C. R. Bunt, S. Ray and A. Seyfoddin, A 3D printed chitosan-pectin hydrogel wound dressing for lidocaine hydrochloride delivery, *Mater. Sci. Eng., C*, 2019, **104**, 109873, DOI: 10.1016/j.msec.2019.109873.

 © 2025 The Author(s). Published by the Royal Society of Chemistry

Open Access Article. Published on 22 August 2025. Downloaded on 11/16/2025 4:40:19 AM.
This article is licensed under a Creative Commons Attribution-NonCommercial 3.0 Unported Licence.

28 M. Kumar, M. Tomar, V. Saurabh, T. Mahajan, S. Punia, M. Contreras, M. del, S. G. Rudra, C. Kaur and J. F. Kennedy, Emerging trends in pectin extraction and its anti-microbial functionalization using natural bioactives for application in food packaging, *Trends Food Sci. Technol.*, 2020, **105**, 223–237, DOI: 10.1016/j.tifs.2020.09.009.

29 C. Nunes, L. Silva, A. P. Fernandes, R. P. F. Guiné, M. R. M. Domingues and M. A. Coimbra, Occurrence of cellobiose residues directly linked to galacturonic acid in pectic polysaccharides, *Carbohydr. Polym.*, 2012, **87**(1), 620–626, DOI: 10.1016/j.carbpol.2011.08.027.

30 S. Y. Chan, W. S. Choo, D. J. Young and X. J. Loh, Pectin as a rheology modifier: origin, structure, commercial production and rheology, *Carbohydr. Polym.*, 2017, **161**, 118–139, DOI: 10.1016/j.carbpol.2016.12.033.

31 G. Wang, H. Li, X. Shao, S. Teng and Q. Wu, Design and development of pH-responsive levofloxacin-loaded metal-organic framework for the promising treatment of pediatric abdominal wound repair, *Regener. Ther.*, 2024, **26**, 170–179, DOI: 10.1016/j.reth.2024.05.003.

32 K. Elkhoury, M. Morsink, L. Sanchez-Gonzalez, C. Kahn, A. Tamayol and E. Arab-Tehrany, Biofabrication of natural hydrogels for cardiac, neural, and bone tissue engineering applications, *Bioact. Mater.*, 2021, **6**(11), 3904–3923, DOI: 10.1016/j.bioactmat.2021.03.040.

33 A. M. J. Coenen, K. V. Bernaerts, J. A. W. Harings, S. Jockenhoevel and S. Ghazanfari, Elastic materials for tissue engineering applications: natural, synthetic, and hybrid polymers, *Acta Biomater.*, 2018, **79**, 60–82, DOI: 10.1016/j.actbio.2018.08.027.

34 N. El Fihry, K. El Mabrouk, M. Eeckhout, H. A. Schols, Y. Filali-Zegzouti and H. Hajjaj, Physicochemical and functional characterization of pectin extracted from Moroccan citrus peels, *LWT*, 2022, **162**, 113508, DOI: 10.1016/j.lwt.2022.113508.

35 S. C. Teixeira, N. O. Gomes, T. V. Oliveira, P. Fortes-Da-Silva, N. F. Soares and P. A. Raymundo-Pereira, Review and perspectives of sustainable, biodegradable, eco-friendly and flexible electronic devices and (Bio)sensors, *Biosens. Bioelectron.: X*, 2023, **14**, 100371, DOI: 10.1016/j.biosx.2023.100371.

36 A. Alam, Y. Zhang, H. C. Kuan, S. H. Lee and J. Ma, Polymer composite hydrogels containing carbon nanomaterials—Morphology and mechanical and functional performance, *Prog. Polym. Sci.*, 2018, **77**, 1–18, DOI: 10.1016/j.progpolymsci.2017.09.001.

37 N. Safitri, N. Rauf and D. Tahir, Enhancing drug loading and release with hydroxyapatite nanoparticles for efficient drug delivery: a review synthesis methods, surface ion effects, and clinical prospects, *J. Drug Delivery Sci. Technol.*, 2023, **90**, 105092, DOI: 10.1016/j.jddst.2023.105092.

38 Y. Yao, A. Zhang, C. Yuan, X. Chen and Y. Liu, Recent trends on burn wound care: hydrogel dressings and scaffolds, *Biomater. Sci.*, 2021, **9**(13), 4523–4540, DOI: 10.1039/D1BM00411E.

39 T. Saravanan, J. M. Pan, F. G. Zingl, M. K. Waldor, Y. Zheng, H. A. Khalil and S. J. Mentzer, Pectin hydrogels as structural platform for antibacterial drug delivery, *Polymers*, 2024, **16**(22), 3202, DOI: 10.3390/polym16223202.

40 C. Xu, Q. Ban, W. Wang, J. Hou and Z. Jiang, Novel nano-encapsulated probiotic agents: encapsulate materials, delivery, and encapsulation systems, *J. Controlled Release*, 2022, **349**, 184–205, DOI: 10.1016/j.jconrel.2022.06.061.

41 X. Wang, Q. Li, Z. Liu, Y. Wu, Z. Zhang, J. Mao and S. Gong, Thermosensitive composite hydrogel with antibacterial, immunomodulatory, and osteogenic properties promotes periodontal bone regeneration *via* staged release of doxycycline and proanthocyanidin, *Mater. Today Chem.*, 2024, **38**, 102052, DOI: 10.1016/j.mtchem.2024.102052.

42 M. A. U. R. Qureshi, N. Arshad, A. Rasool, M. Rizwan, K. F. Fawy and T. Rasheed, pH-responsive chitosan dendrimer hydrogels enabling controlled cefixime release, *Eur. Polym. J.*, 2024, **219**, 113377, DOI: 10.1016/j.eurpolymj.2024.113377.

43 M. A. U. R. Qureshi, N. Arshad, A. Rasool, N. K. Janjua, M. Shoaib, M. Naqeeb Ur Rehman and H. Ismail, Kappa-carrageenan and sodium alginate-based pH-responsive hydrogels for controlled release of methotrexate, *R. Soc. Open Sci.*, 2024, **11**(4), 231952, DOI: 10.1098/rsos.231952.

44 D. Demir, S. Ceylan, D. Göktürk and N. Bölgen, Extraction of pectin from albedo of lemon peels for preparation of tissue engineering scaffolds, *Polym. Bull.*, 2021, **78**, 2211–2226, DOI: 10.1007/s00289-020-03208-1.

45 G. Acik, M. Kamaci, B. ÖZATA and C. Cansoy, Effect of polyvinyl alcohol/chitosan blend ratios on morphological, optical, andthermal properties of electrospun nanofibers, *Turk. J. Chem.*, 2019, **43**, 137–149, DOI: 10.3906/kim-1801-68.

46 V. C. Karade, A. Sharma, R. P. Dhavale, S. R. Shingte, P. S. Patil, J. H. Kim, D. R. T. Zahn, A. D. Chougale, G. Salvan and P. B. Patil, APTES monolayer coverage on self-assembled magnetic nanospheres for controlled release of anticancer drug Nintedanib, *Sci. Rep.*, 2021, **11**(1), 5674, DOI: 10.1038/s41598-021-84770-0.

47 O. Kesmez, Preparation of anti-bacterial biocomposite nanofibers fabricated by electrospinning method, *J. Turk. Chem. Soc. Sect., A Chem.*, 2019, **7**, 125–142, DOI: 10.18596/jotcsa.590621.

48 S. Hafeez, A. Islam, A. K. Durrani, M. T. Z. Butt, S. Rehmat, A. Khurshid and S. M. Khan, Fabrication of pectin-based stimuli responsive hydrogel for the controlled release of ceftriaxone, *Chem. Pap.*, 2023, **77**(4), 1809–1819, DOI: 10.1007/s11696-022-02495-4.

49 S. M. Hosseini, R. Abbasalipourkabir, F. A. Jalilian, S. S. Asl, A. Farmany, G. Roshanaei and M. R. Arabestani, Doxycycline-encapsulated solid lipid nanoparticles as promising tool against Brucella melitensis enclosed in macrophage: a pharmacodynamics study on J774A.1 cell line, *Antimicrob. Resist. Infect. Control*, 2019, **8**, 62, DOI: 10.1186/s13756-019-0504-8.

50 D. Gawkowska, J. Cybulska and A. Zdunek, Structure-related gelling of pectins and linking with other natural

Open Access Article. Published on 22 August 2025. Downloaded on 11/16/2025 4:40:19 AM.
This article is licensed under a Creative Commons Attribution-NonCommercial 3.0 Unported Licence.

compounds: a review, *Polymers*, 2018, **10**(7), 762, DOI: 10.3390/polym10070762.

51 S. Bashir, N. Zafar, N. Lebaz, A. Mahmood and A. Elaissari, Hydroxypropyl methylcellulose-based hydrogel copolymeric for controlled delivery of galantamine hydrobromide in dementia, *Processes*, 2020, **8**(11), 1350, DOI: 10.3390/pr8111350.

52 M. Wu, H. Ping, K. Wang, H. Ding, M. Zhang, Z. Yang and Q. Du, Oral delivery of pectin-chitosan hydrogels entrapping macrophage-targeted curcumin-loaded liposomes for the treatment of ulcerative colitis, *Int. J. Pharm.*, 2023, **647**, 123510, DOI: 10.1016/j.ijpharm.2023.123510.

53 A. Zarinwall, T. Waniek, R. Saadat, U. Braun, H. Sturm and G. Garnweitner, Comprehensive characterization of APTES surface modifications of hydrous boehmite nanoparticles, *Langmuir ACS J. Surf. Colloids*, 2021, **37**(1), 171–179, DOI: 10.1021/acs.langmuir.0c02682.

54 Y. Hu, B. Yu, Y. Jia, M. Lei, Z. Li, H. Liu, H. Huang, F. Xu, J. Li and Z. Wei, Hyaluronate- and gelatin-based hydrogels encapsulating doxycycline as a wound dressing for burn injury therapy, *Acta Biomater.*, 2023, **164**, 151–158, DOI: 10.1016/j.actbio.2023.04.021.

55 X. Zhao, Y. Yang, J. Yu, R. Ding, D. Pei, Y. Zhang, G. He, Y. Cheng and A. Li, Injectable hydrogels with high drug loading through B–N coordination and ROS-triggered drug release for efficient treatment of chronic periodontitis in diabetic rats, *Biomaterials*, 2022, **282**, 121387, DOI: 10.1016/j.biomaterials.2022.121387.

56 M. A. U. R. Qureshi, N. Arshad and A. Rasool, Graphene oxide reinforced biopolymeric (chitosan) hydrogels for controlled cephradine release, *Int. J. Biol. Macromol.*, 2023, **242**, 124948, DOI: 10.1016/j.ijbiomac.2023.124948T.

57 N. Batool, R. M. Sarfraz, A. Mahmood, U. Rehman, M. Zaman, S. Akbar, D. M. Almasri and H. A. Gad, Development and evaluation of cellulose derivative and pectin based swellable ph responsive hydrogel network for controlled delivery of cytarabine, *Gels*, 2023, **9**, 60, DOI: 10.3390/gels9010060.

58 L. G. da Trindade, G. Y. Hata, J. C. Souza, M. R. S. Soares, E. R. Leite, E. C. Pereira, E. Longo and T. M. Mazzo, Preparation and characterization of hematite nanoparticles-decorated zinc oxide particles (ZnO/Fe_2O_3) as photoelectrodes for solar cell applications, *J. Mater. Sci.*, 2020, **55**(7), 2923–2936, DOI: 10.1007/s10853-019-04135-x.

59 M. A. U. R. Qureshi, N. Arshad, A. Rasool, M. Rizwan and T. Rasheed, Guar gum-based stimuli responsive hydrogels for sustained release of diclofenac sodium, *Int. J. Biol. Macromol.*, 2023, **250**, 126275, DOI: 10.1016/j.ijbiomac.2023.126275.

60 J. S. Lee, K. H. Sun and Y. Park, Evaluation of Melia azedarach extract-loaded poly(vinyl alcohol)/pectin hydrogel for burn wound healing, *PLoS ONE*, 2022, **17**(6), e0270281, DOI: 10.1371/journal.pone.0270281.

61 J. Li, C. Peng, A. Mao, M. Zhong and Z. Hu, An overview of microbial enzymatic approaches for pectin degradation, *Int. J. Biol. Macromol.*, 2024, **254**(Pt 1), 127804, DOI: 10.1016/j.ijbiomac.2023.127804.

62 C. Lara-Espinoza, E. Carvajal-Millán, R. Balandrán-Quintana, Y. López-Franco and A. Rascón-Chu, Pectin and pectin-based composite materials: beyond food texture, *Molecules*, 2018, **23**(4), 942, DOI: 10.3390/molecules23040942.

63 A. S. MK, S. Hadi, Y. W. Sari, N. Cahyati, Y. Yusuf and C. A. C. Abdullah, Fabrication and biocompatibility evaluation of hydroxyapatite–polycaprolactone–gelatin composite nanofibers as a bone scaffold, *RSC Adv.*, 2024, **14**(34), 24815–24827, DOI: 10.1039/D4RA02485K.

64 F. Souza Almeida, K. C. Guedes Silva, A. Matias Navarrete de Toledo and A. C. Kawazoe Sato, Modulating porosity and mechanical properties of pectin hydrogels by starch addition, *J. Food Sci. Technol.*, 2021, **58**(1), 302–310, DOI: 10.1007/s13197-020-04543-x.

65 B. Zhao, M. Zhao, L. Li, S. Sun, H. Yu, Y. Cheng, Y. Yang, Y. Fan and Y. Sun, Preparation and properties of double-crosslinked hydroxyapatite composite hydrogels, *Int. J. Mol. Sci.*, 2022, **23**(17), 9962, DOI: 10.3390/ijms23179962.

66 F. V. Lavrentev, V. V. Shilovskikh, V. S. Alabusheva, V. Yu. Yurova, A. A. Nikitina, S. A. Ulasevich and E. V. Skorb, Diffusion-limited processes in hydrogels with chosen applications from drug delivery to electronic components, *Molecules*, 2023, **28**(15), 5931, DOI: 10.3390/molecules28155931.

67 S. Nandi, R. Swain, S. Habibullah, R. N. Sahoo, A. K. Nayak and S. Mallick, Lipid-Gelucire based rectal delivery of ramipril prodrug exhibits significant lowering of intra-ocular pressure in normotensive rabbit: sustained structural relaxation release kinetics and IVIVC, *Pharm. Dev. Technol.*, 2024, **29**(5), 468–476, DOI: 10.1080/10837450.2024.2345807.

68 S. Habibullah, R. Swain, S. Nandi, M. Das, T. Rout, B. Mohanty and S. Mallick, Nanocrystalline cellulose as a reinforcing agent for poly(vinyl alcohol)/gellan-gum-based composite film for moxifloxacin ocular delivery, *Int. J. Biol. Macromol.*, 2024, **270**(1), 132302, DOI: 10.1016/j.ijbiomac.2024.132302.

69 H. Kaçoğlu, O. Ceylan and M. Çelebi, Determination of swelling kinetics and diffusion mechanisms of chemically crosslinked porous chitosan hydrogels, *Open J. Nano*, 2024, **9–2**, 106–118, DOI: 10.56171/ojn.1488770.

70 M. Rizwan, R. Yahya, A. Hassan, M. Yar, A. D. Azzahari, V. Selvanathan, F. Sonsudin and C. N. Abouloula, pH sensitive hydrogels in drug delivery: brief history, properties, swelling, and release mechanism, material selection and applications, *Polymers*, 2017, **9**(4), 137, DOI: 10.3390/polym9040137.

71 R. Wang, C. Cheng, H. Wang and D. Wang, Swollen hydrogel nanotechnology: advanced applications of the rudimentary swelling properties of hydrogels, *ChemPhysMater*, 2024, **3**(4), 357–375, DOI: 10.1016/j.chphma.2024.07.006.

72 A. Rasool, S. Ata, A. Islam and R. Ullah Khan, Fabrication of novel carrageenan based stimuli responsive injectable

 © 2025 The Author(s). Published by the Royal Society of Chemistry

Open Access Article. Published on 22 August 2025. Downloaded on 11/16/2025 4:40:19 AM.
This article is licensed under a Creative Commons Attribution-NonCommercial 3.0 Unported Licence.

hydrogels for controlled release of cephradine, *RSC Adv.*, 2019, **9**(22), 12282–12290, DOI: 10.1039/C9RA02130B.

73 D. Aydınoğlu, Investigation of pH-dependent swelling behavior and kinetic parameters of novel poly(acrylamide-co-acrylic acid) hydrogels with spirulina, *E-Polymers*, 2015, **15**(2), 81–93, DOI: 10.1515/epoly-2014-0170.

74 F. Ahadi, S. Khorshidi and A. Karkhaneh, A hydrogel/fiber scaffold based on silk fibroin/oxidized pectin with sustainable release of vancomycin hydrochloride, *Eur. Polym. J.*, 2019, **118**, 265–274, DOI: 10.1016/j.eurpolymj.2019.06.001.

75 D. U. Kapoor, R. Garg, M. Gaur, A. Pareek, B. G. Prajapati, G. R. Castro, S. Suttiruengwong and P. Sriamornsak, Pectin hydrogels for controlled drug release: recent developments and future prospects, *Saudi Pharm. J.*, 2024, **32**(4), 102002, DOI: 10.1016/j.jsps.2024.102002.

76 N. H. Thang, T. B. Chien and D. X. Cuong, Polymer-based hydrogels applied in drug delivery: an overview, *Gels*, 2023, **9**(7), 523, DOI: 10.3390/gels9070523.

77 P. Kavish, R. Kalpana and V. Kumar, Doxycycline drug release property of glutaraldehyde crosslinked hydrogel, *J. Pharm. BioAllied Sci.*, 2024, **16**(Suppl 2), S1204–S1206, DOI: 10.4103/jpbs.jpbs_541_23.

78 D. Stan, L. L. Ruta, L. A. Bocancia-Mateescu, A. C. Mirica, D. Stan, M. Micutz, O. Brincoveanu, A. M. Enciu, E. Codrici, I. D. Popescu, M. L. Popa, F. Rotaru and C. Tanase, Formulation and comprehensive evaluation of biohybrid hydrogel membranes containing doxycycline or silver nanoparticles, *Pharmaceutics*, 2023, **15**(12), 2696, DOI: 10.3390/pharmaceutics15122696.

79 O. Saliy, M. Popova, H. Tarasenko and O. Getalo, Development strategy of novel drug formulations for the delivery of doxycycline in the treatment of wounds of various etiologies, *Eur. J. Pharm. Sci.*, 2014, **195**, 106636, DOI: 10.1016/j.ejps.2023.106636.

80 I. Y. Wua, S. Balaa, N. Š. Basneta and M. P. di Cagno, Interpreting non-linear drug diffusion data: utilizing Korsmeyer-Peppas model to study drug release from liposomes, *Eur. J. Pharm. Sci.*, 2019, **138**, 105026, DOI: 10.1016/j.ejps.2019.105026.

81 A. N. F. Marzaman, U. Mahfufah, N. Fauziah, F. Ulum Ar Rahman, N. Hidayati, R. Hasyim, D. Setiawati, S. Choiri, N. A. Nuzulia, A. F. Madani, M. Mir, A. D. Permana and K. Q. Mansjur, Doxycycline-loaded pH-sensitive microparticles as a potential site-specific drug delivery system against periodontitis, *ACS Omega*, 2025, **10**(6), 5668–5685, DOI: 10.1021/acsomega.4c08967.

82 M. Pandey, H. Choudhury, S. K. Segar Singh, N. Chetty Annan, S. K. Bhattamisra, B. Gorain and M. C. I. Mohd Amin, Budesonide-loaded pectin/polyacrylamide hydrogel for sustained delivery: fabrication, characterization and *in vitro* release kinetics, *Molecules*, 2021, **26**(9), 2704, DOI: 10.3390/molecules26092704.

83 K. Aliyeva, A. Albayrak, E. Toktay, E. E. Yurdgulu and Y. Bayir, The role of pectin hydrogel systems plus iodine and phyto extract in second-degree burn in rats, *Eurasian J. Med.*, 2024, **56**(3), 170–177, DOI: 10.5152/eurasianjmed.2024.24550.

84 M. Rezvanian, N. Ahmad, M. C. I. Mohd Amin and S. F. Ng, Optimization, characterization, and *in vitro* assessment of alginate-pectin ionic cross-linked hydrogel film for wound dressing applications, *Int. J. Biol. Macromol.*, 2017, **97**, 131–140, DOI: 10.1016/j.ijbiomac.2016.12.079.

85 U. Farghaly Aly, H. A. Abou-Taleb, A. A. Abdellatif and N. Sameh Tolba, Formulation and evaluation of simvastatin polymeric nanoparticles loaded in hydrogel for optimum wound healing purpose, *Drug Des., Dev. Ther.*, 2019, **13**, 1567–1580, DOI: 10.2147/DDDT.S198413.